Effects of shade and deficit irrigation on maize growth and development in fixed and dynamic AgriVoltaic systems

Isaac A Ramos-Fuentes, Yassin Elamri, Bruno Cheviron, Cyril Dejean, Gilles Belaud, Damien Fumey

Agricultural Water Management 280 (2023) 108187

Contents lists available at ScienceDirect

Agricultural Water Management

journal homepage: www.elsevier.com/locate/agwat

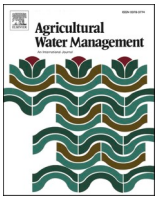

Effects of shade and deficit irrigation on maize growth and development in fixed and dynamic AgriVoltaic systems

Isaac A. Ramos-Fuentes [a,b,*], Yassin Elamri [b], Bruno Cheviron [a], Cyril Dejean [a], Gilles Belaud [a], Damien Fumey [b]

[a] UMR G-Eau, INRAE, Institut Agro, Univ. Montpellier, 361 Rue Jean François Breton, 34196 Montpellier, France
[b] Sun'Agri, 45 allée Yves Stourdzé, 34830 Clapiers, France

ARTICLE INFO

Handling Editor - Dr R Thompson

Keywords:
AgriVoltaic systems
Maize
Shading
Deficit irrigation
Crop production

ABSTRACT

Maize production is essential for global food security and represents a major supply in several value chains. However, the projected effects of climate change are likely to decrease drastically water availability for crops in many regions, affecting yield. AgriVoltaics (AV) systems are an innovative solution that may improve maize resilience in water-scarce regions mainly by protecting plants from excessive radiation and by reducing irrigation needs. However, shade from panels may also affect crop development and production. This study addresses the interplay between radiation transmission, crop development and irrigation needs of maize cropping in field conditions, by the description of crop development dynamics, distinguishing between fixed and dynamic panels. We showed that maize crop responded to both independent and combined stresses (shade and water deficit), with a significant decrease in leaf area index, total dry matter and grain yield. Concerning water use, we showed the potential of AV to reduce irrigation inputs (by up to 19–47% compared to unshaded plots) via reduced soil water depletion and reference evapotranspiration. The crop development was impacted by shade by increasing phyllochron and causing a generalized delay in phenology. At a finer temporal scale, we concluded that maize leaves react to shade by reducing stomatal conductance, net assimilation of CO_2 and leaf temperature in a correlated way to radiation, opening the possibility to use this behavior to optimize water use and shading strategies. The spatial heterogeneities of radiation in fixed AV systems, compared to dynamic AV systems, were identified as a second-order effect at the plot level on leaf area index and phyllochron, compared to the effect of radiation reduction. Moreover, dynamic AV showed their ability to reduce the spatial heterogeneities in soil water depletion, showing the importance of controlled shade strategies in AV systems concerning water use.

1. Introduction

Maize is one of the most important cereals in the world together with rice and wheat, currently produced on nearly 55 million hectares in 174 countries (FAOSTAT, 2022). Its production is essential for global food security and represents a primary source of food in several countries worldwide, mainly in Latin America, Asia and Africa (Poehlman, 2013) due to their irreplaceable nutritional content, playing at the same time an important role in the livelihoods of millions of poor farmers. From an economical point of view, maize grain and its derivatives provide raw materials for industry (oil, fibers, fermentable sugars, starch, etc.) and their supply is important for several value chains, particularly for global food supply chains (agro-industry, livestock), representing a major component of the export trade in some countries and regions. However, the world population is expected to reach 9.7 billion in 2050, 1.8 billion more than at present (Foley et al., 2011), creating a serious risk of shortage of grain supply considering the existing land resources and cereal production capacity (Tilman et al., 2002). Additionally, it is anticipated that the effects of climate change will drastically impact food production, reducing water availability and raising crop water needs, affecting crop development and yield (Reilly, 2002). Projected increase in temperatures, more recurrent soil moisture droughts (Grillakis, 2019), high inter-annual and seasonal climatic variability, and the potential increase of water withdrawals constraints (Shen et al., 2008) will have significant negative effects on maize production (Basso and Ritchie, 2014). Even if maize has an efficient use of water, high yields require between 500 and 800 mm of water per season (depending on the climate), making it necessary to provide irrigation in many regions of

* Corresponding author at: UMR G-Eau, INRAE, Institut Agro, Univ. Montpellier, 361 Rue Jean François Breton, 34196 Montpellier, France.
E-mail address: arturo.ramosfuentes@sunagri.fr (I.A. Ramos-Fuentes).

https://doi.org/10.1016/j.agwat.2023.108187
Received 26 October 2022; Received in revised form 26 December 2022; Accepted 20 January 2023
Available online 7 February 2023

the world. Conversely, global cereal production on irrigated land would decrease by 47% without irrigation supply, corresponding to a loss of around 20% of the total cereal production (Siebert and Döll, 2010). Additionally, models reveal that climate changes could increase the net irrigation water requirement of maize by up to 20% in 2080, depending on the region (Oumarou Abdoulaye et al., 2019). This should exacerbate the already high tensions on water resources, particularly in water-scarce regions.

AgriVoltaics (AV) systems are an innovative solution that would make it possible to grow crops while preserving land resources and producing renewable energy (Mamun et al., 2022). Since the first agrivoltaic experiments were performed in France (Marrou et al., 2013a; Marrou et al., 2013b), AV systems have proven their capacity to protect crops face to some climatic hazards, particularly by intercepting radiations that would be excessive for the crops (Wang and Sun, 2018) and by improving the resilience of cropping systems to climate variability (Amaducci et al., 2018). AV systems also represent a potential way to save water by reducing irrigation needs due to the decrease of evapotranspiration (Elamri et al., 2018; Barron-Gafford et al., 2019; AL-agele et al., 2021).

Various types of AV systems have been developed; the most common with fixed panels only mounted over the crop (fixed AV). More recently, structures integrating sophisticated tracking systems (dynamic AV or DAV) have made it possible to control the movement of panels, generally to maximize energy production by maintaining direct exposure of the panels to the sun. Rotation of panels can be thought to optimize radiation available for the crop grown under the panels (Valle, 2017), this being one of the principal agronomic advantages of dynamic AV compared to fixed AV for crop production (Tahir and Butt, 2022). However, the magnitude and spatiotemporal patterns of shading should be examined in detail in AV, distinguishing between fixed and dynamic systems. Particularly as the temporal patterns of transmitted radiation to crops under dynamic AV take place over the short-term (with characteristic times of a few minutes) and short distances (with characteristic lengths of a few centimeters) when following the movements of the panels, modifying and complexifying the spatial characteristics of crop environment (compared to full-sun conditions or fixed AV).

Despite the above advantages, solar panels also “compete” with plants for radiation, which can affect crop growth and production. High shading during sensitive phenological stages of maize negatively affects dry matter (Reed et al., 1988), yield components and grain quality (Andrade and Ferreiro, 1996; Earley et al., 1966; Jia et al., 2011), leaf and shoot growth and morphology (Ephrath et al., 1993; Gao et al., 2017; Yuan et al., 2021). There are no detailed studies carried out on AV to evaluate their agronomical impacts on maize crop dynamics (phenology, soil water depletion, leaf expansion, biomass production, photosynthesis, and transpiration). Agroforestry research has explored the impact of shaded environments, but the differences in the nature of shading, and its temporal variability, in these systems make it difficult to extrapolate the results to AV (in agroforestry characterized by irregular and porous shade associated with the canopy cover while in AV characterized by regular and not porous shade).

The influence of AV on soil water balance has already been studied for various irrigated crops such as fruit trees and some cereals (Mamun et al., 2022). For maize, a crop particularly sensitive to the effect of soil water content on yield, the potential of AV to manage water stress remains to explore. Also, considering the extensive worldwide range of water conditions of maize cropping, these systems must be assessed under drought or deficit irrigation strategies, considering erratic rainfall, extreme weather, or irrigation shortages. Particularly, deficit (or regulated deficit) irrigation is one strategy for maximizing yields per unit of irrigation water applied to several crops including maize (Huang et al., 2011; Zou et al., 2021).

To remedy the current lack in the literature, this paper essentially tackles the interplay between radiation transmission, crop development and irrigation needs of maize cropping in field conditions. This is done through the description of crop development dynamics and crop indicators, as well as the differences of this interplay between fixed and dynamic AV systems, comparing them with control case (full-sun). Based on experiments, we analyze contrasting situations in terms of shading conditions (by different AV devices generating different shading spatial and temporal patterns) and water conditions (irrigation treatments). The aim is to create a knowledge base for further studies of the complementary controls (piloting of the shade and piloting of irrigation) and their optimization in terms of water consumption, energy production and crop development, which are known to be partially conflicting goals.

2. Materials and methods

2.1. Site description and environmental conditions

This study was conducted in the South of France (Mediterranean climate). Maize crop (*Zea mays L.*, RAGT IXABEL) was grown for three years (2019, 2020 and 2021) in the agrivoltaic experimental platform of Lavalette (INRAE Montpellier, France: 43.6466°N; 3.8715°E), covering an area of 1720 m^2 (Fig. 1). Sowing in the 2020 and 2021 seasons took place on April 2 and April 16, respectively, while in 2019 sowing took place on May 3. The length of the seasons was of 138, 144 and 152 days, for 2019, 2020 and 2021 respectively. Sowing and harvest were done at the same date for all treatments each season. The environmental conditions during the three cropping seasons were characterized by daily averaged values of five relevant meteorological variables measured in FULLSUN plot: Air temperature (T_{air}), Relative Humidity of the air (*RH*), Incident Global Radiation (*Rg*), Reference Evapotranspiration (*ETo*) and Rainfall (*R*) (supplementary Fig. S1). The total amount of rainfall was modified in AV plots by using the methodology showed by Elamri et al. (2018b) to consider the effect of panels in rainfall interception. Daily air temperatures varied between 12 and 31 °C in 2019, between 10 and 28 °C in 2020 and between 9 and 27 °C in 2021. The 2019 and 2021 seasons were characterized by more overcast days (particularly in 2021), while 2020 was characterized by cloudy days observed at the beginning of the cropping season and mostly sunny days during the irrigation period. Rainfall during the cropping periods amounted to 150, 264 and 324 mm, in 2019, 2020 and 2021 respectively. This, coupled with the fact that rainfall events were mainly out of the irrigation period in 2019 and 2020, indicates that in 2021 experiments occurred in a rainy season, whereas in 2019 and 2020 during dry conditions. Typical cultural practices have been adopted in a similar way during the three cropping seasons. Sufficient nitrogen amounts have been delivered to all plots (during sowing) to prevent nitrogen stress conditions.

2.2. Experimental platform characteristics and experimental design

The platform is composed of four AV plots with photovoltaic panels held at 4 m above the ground, resulting in different incoming radiation conditions for the crops. The two fixed-tilt AV plots “AVfull” and “AVhalf” (without tracker systems), consist of monocrystalline photovoltaic panels (1.58 ×0.81 m) installed with a fixed tilt angle of 25° with respect to the horizontal plane and aligned in strips of 22.4 m, oriented in the east-west direction. The “AVfull” plot corresponds to the full density of panels (as in optimal design for a solar energy production plant) producing a shading rate of approx. 50% (reduction of 50% of total global radiation available for the crop in the plot surface during a day). The “AVhalf” consists of the same design of “AVfull” plot but with the half density of panels (one row of panels removed out of two) to limit radiation reduction, producing a shading rate of approx. 30%. The two 1-axis dynamic AV plots, called “DAV” (Dynamic AgriVoltaics) were added in 2014 on the eastern and western sides of the fixed subsystem, with 3 and 4 strips, respectively. Each strip in DAV consists of monocrystalline photovoltaic panels (1.98 ×1.00 m) aligned in 19 m long strips and oriented in the north-south direction. The strips are

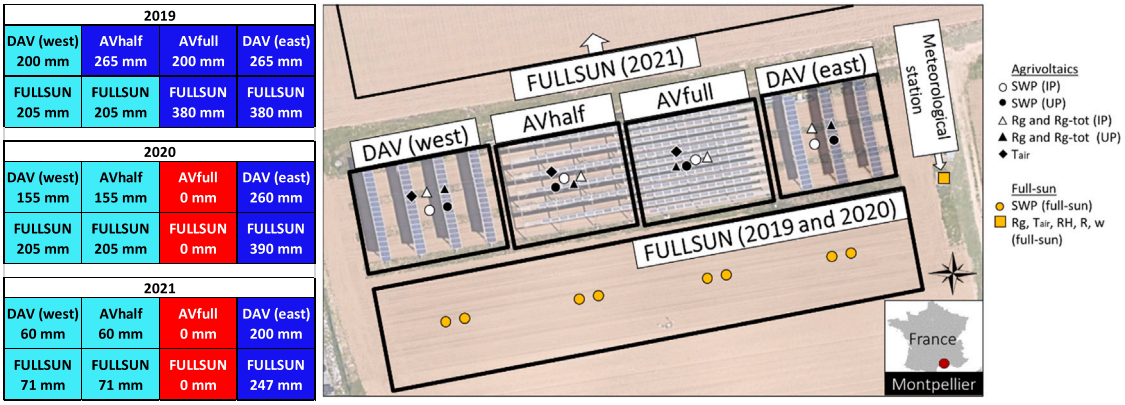

Fig. 1. Experimental agrivoltaic site of Lavalette (Montpellier, France): maps of the experiments (left) and view from above (right). The map on the left depicts the location of the different plots during the three seasons, indicating the total amount of the applied irrigation (in mm). The colors represent the different irrigation treatments: dark-blue for fully irrigated (FI), light-blue for deficit irrigated (DI), red for not irrigated (NI). In the view from above, the symbols indicate the location of measurement devices: circles = Soil Water Potential (*SWP*) at 30–60–90–120 cm depths; triangles = Incident Global Radiation (*Rg*) and Total Global Radiation (Rg-tot*);* diamonds = Air Temperature (T_{air}) and Relative Humidity of the air (*RH*). White-filled symbols indicate Inter-Panels position (IP) and black-filled symbols indicate Under-Panels positions (UP) in AV plots. Yellow-filled symbols indicate the sensors in FULLSUN conditions. The yellow-filled square indicates the position of the meteorological station, at the east of the plots, collecting multiple variables: *Rg*, T_{air}, *RH* and *R* in FULLSUN conditions. During the 2019 and 2020 seasons, the FULLSUN plots were located south of the AV platform. During the 2021 season, FULLSUN plots were located north of AV platform, because of a germination issue in the conventional 2019–2020 FULLSUN plots. The FULLSUN plots in 2021 are not visible in the above view, but the instrumentation corresponds to that of the 2019 and 2020 FULLSUN plots.

electrically controlled according to a horizontal axis rotation strategy thought to maximize radiation interception by the photovoltaic panels. This strategy consists of the panels' faces following the course of the sun by varying the tilt angle of the strips between 50°E and 50°W. The resulting shading rate in DAV devices is about 35%, which is similar to the AVhalf structure, but with different subscale patterns regarding the drop shadows of the panels in space and time. The control plot without panels is called "FULLSUN" (representing a shading rate of 0%). It covers an area of 1760 m^2 and is located immediately south of the AV plots, without being affected by the shadow generated by the panels. More details about the AV platform of Lavalette were described by Elamri et al. (2018).

Depending on the season, the shading conditions have been crossed with three different irrigation treatments: Fully Irrigated Treatment (FI), Deficit Irrigated Treatment (DI), and Not Irrigated Treatment (NI). FI plots were irrigated when soil water potential dropped to − 80 kPa (comfort limit for the silt-sandy soil texture of the site) based on tensiometer readings (Watermark probes, IRROMETER Company, Riverside, USA) at different depths, considering the dynamics of root water uptake and based on 30 cm readings between 60 and 80 days after sowing (DAS), on the mean of 30–60 cm between 80 and 100 DAS and on mean of 30–60–90 cm from 100 DAS until the end of irrigations (around 120 DAS). DI plots were irrigated between − 120 kPa to − 150 kPa soil water potential range to induce moderate water stress. The irrigation periods took place during DAS 55–112 (57 days), 69–122 (53 days) and 52–126 (74 days), in 2019, 2020 and 2021, respectively. Water was applied using an integral sprinkler system in fixed amounts of 40 mm (to fill the soil water reserve of the first 30 cm and prevent water loss by deep percolation). In AV irrigated plots the amount was multiplied by 0.7 (amounts of 28 mm) in order to adapt to the approx. 30% radiation reduction in DAV and AVhalf. The pipes were installed each year before the irrigation period and removed before harvest. Irrigation applications to each treatment were measured with calibrated mechanical flow meters for each plot. Uniform water distribution among plots was ensured by a constant pressure water supply in a relatively flat topography, controlled with a variable speed drive booster pump and control pressure valves. Table 1 shows the experimental design matrix, indicating the level of combined stress and the variables studied for each cropping season.

Table 1
Experimental design table for the factors (shade and irrigation) and responses monitored, varying slightly between the three cropping seasons. The symbols in the stress column indicate the level of stress: • = moderate shade (shading rate around 30–35%); •• = high shade (shading rate around 50%); ┼ = deficit irrigated (−120 kPa to −150 kPa) ; ┼┼ = not irrigated. The * indicates that in 2020 only flowering was monitored (not leaf number). The letter after the shade factor indicates: D = Dynamic-tilt device and F = Fixed-tilt device.

Shade		Irrigation	Stress	2019	2020	2021
FULLSUN		FI	Control (no stress)	✓	✓	✓
FULLSUN		DI	┼	✓	✓	✓
FULLSUN		NI	┼┼		✓	✓
DAV	D	FI	•	✓	✓	✓
DAV	D	DI	•┼	✓	✓	✓
DAV	D	NI	•┼┼			
AVhalf	F	FI	•	✓		
AVhalf	F	DI	•┼		✓	✓
AVhalf	F	NI	•┼┼			
AVfull	F	FI	••	✓		
AVfull	F	DI	••┼			
AVfull	F	NI	••┼┼		✓	✓
Crop growth and production (*LAI*, *TDM* and *GY*)				✓	✓	✓
Climate and soil water monitoring (*Rg*, T_{air}, *SWP*)				✓	✓	✓
Phenology (Leaf number and flowering)					✓*	✓

2.3. Climate and soil water potential monitoring

Microclimate data were recorded with a 10-min time step at a height of 2 m: a weather station was installed close to the FULLSUN plot: the Air Temperature (T_{air}) and Relative Humidity of the air (*RH*) by digital thermo-hygrometer (CS215, Campbell Sci. Inc.); Incident Global Radiation (*Rg*) and Total Global Radiation (Rg-tot, *that is a cumulated measure of* Rg *in a period) by* pyranometer (SP1110 Campbell Sci. Inc.); Rain (*R*) by pluviometer (52203, RM Young Company); and Wind Speed (*w*) by an anemometer (05103-L, RM Young Company). Air temperature and global radiation measurements were also made in the AV plots. The thermo-hygrometers in the AV plots were installed in DAV (west) and AVfull plots for the 2019 cropping season and DAV (west) and AVhalf plots for the 2020 and 2021 cropping seasons. The thermo-hygrometers installed in AV plots were installed at a point covered by panels to differentiate from not covered sensors in the weather station installed

for FULLSUN conditions. The pyranometers in AV plots were installed in two different locations, Inter-Panels (IP) and Under-Panels (UP), to capture the differences in the spatial intra-day patterns of radiation transmission under the photovoltaic strips.

Reference Evapotranspiration (*ETo*) was calculated with the FAO#56 equation (Allen et al., 1998) using the recorded data of each plot at a daily timestep. Radiation in AV plots was the average of IP and UP sensors and rainfall amounts were corriged to consider the effect of the panels using the methodology showed by Elamri et al. (2018b). The other variables (relative humidity, air temperature and wind speed), less affected by the solar panels (Marrou et al., 2013a) due to the height of the structure about the crop, were assumed as the same for all treatments and taken from the FULLSUN weather station.

Soil water status was monitored by Soil Water Potential measurements (*SWP*) using soil water potential sensors (Watermark) also recorded every 10-min at 4 depths (30–60–90–120 cm). Since solar panels are likely to cause large heterogeneity on soil moisture after rainfalls (Elamri et al., 2018b), *SWP* was also measured in two positions (IP and UP) for AV plots, similarly to radiation measurements (see Fig. 2).

2.4. Crop phenology, vegetative growth, and production

Plant emergence was characterized by counting the number of visible plants that emerged in 12 rows per treatment, through a determined stripe of 13 m (covering an area of 123 m^2). The emergence stage date was reported when the percentage of emerged plants reached at least 50%. The phenological development of the maize crop was monitored under the different water and radiative conditions by median dates of vegetative stages (leaf number) and flowering stages (tasselling and silking), which corresponded to the date when 50% of the plants reached the stage. The count in vegetative and flowering stages was carried out under each plot and for different rows, in 430 tagged maize plants, covering an average total area of 60 m^2 per plot. Leaf number monitoring was carried out only for the 2021 cropping season from V2 (2-leaf stage) until first visible flowers appeared (n-leaf stage corresponding to final number of leaves) by weekly counting of "deployed leaves", commonly the ligulate leaves for the maize crop (IOWA scale, commonly used in maize studies, as described by Abendroth. et al., 2011). The dates of the reproductive stages were identified in the 2020 and 2021 cropping seasons: tasseling (VT) and silking (R1), starting when at least one extruded anther or one extruded silk was visible in all tagged plants. All the phenology results are presented using plant age time (DAS), commonly used in agronomy.

During the three years of experiments the vegetative growth has been characterized by around 12 weekly measurements of Leaf Area Index (*LAI*), using the LAI-2200 C – LICOR system, from early vegetative development until observing a decrease in *LAI* (after the maximum LAI values), measuring ten values of *LAI* across a parallel central line between two central rows in each plot. Crop production has been estimated at harvest by sampling of 40 tagged plants to estimate the Total Dry Matter (*TDM*) of aerial part only (leaves, stem, ears) and Dry Grain Yield (*GY*) for the three seasons, following standard methods: individual plants sampled without the root were separated into leaves, stem, and ears. The samples were then oven-dried at a constant temperature of 65 °C for 72 h and weighed individually, separating the ears from the leaves and the shoots. Dry kernels were separated from the cob to estimate *GY*. Harvest index values (*HI*) have been calculated as the ratio of *GY* and aerial *TDM* at maturity (Kawano, 1990). Data on *TDM* and *GY* were subjected to analysis of variance (ANOVA) using R package (r-stats) version 2.0. The means were considered different if the p-value was less or equal to 0.05 ($p \leq 0.05$). For all analyses, the normality and the independence of residuals and the intra-treatment variance equality were checked.

Daily Growing Degree-Days (*GDD*, °Cd) were calculated following the classical approach: $GDD = (T_{mean} - T_{base})$, where T_{mean} is the mean air temperature calculated as the daily average of 10-minute recorded data, and T_{base} is the base temperature, assumed 6 °C, as identified for this species in the south of France conditions (Brisson et al., 1992). Then we evaluated the relationships between *GDD* and leaf number, employing the Phyllochron (*PHY*; °Cd/leaf) concept, also rendered as leaf appearance^{-1} (dos Santos et al., 2022a). The *PHY* is used to describe the growth and development of plants (especially cereals) by the relationship between leaf number and thermal time (*GDD* accumulation). We fit linear models to compute phyllochron values, where the slope of the line is the *PHY* for the entire leaf vegetative period. Model fit was assessed by

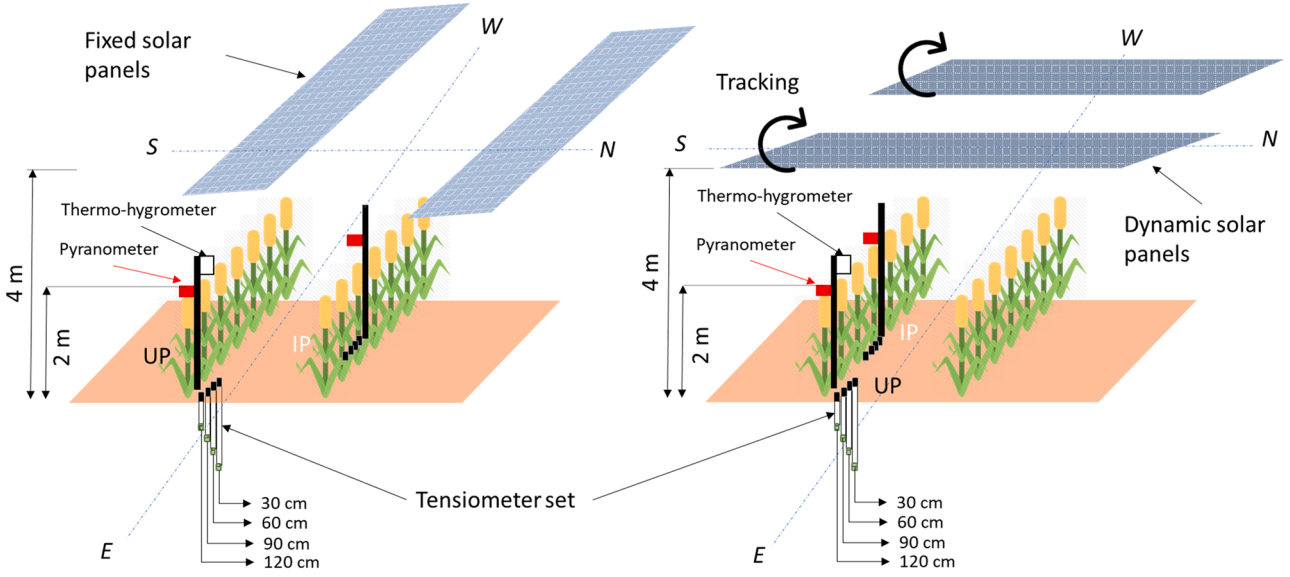

Fig. 2. Scheme of the instrumentation to monitoring radiation, air temperature and soil water potential in the fixed AV plots (on the left) and in dynamic AV plots (on the right). In the fixed AV plots (AVhalf and AVfull), the instrumentation was installed in different maize rows in a way to be placed in two different positions Inter-Panels (IP – between two arrays of solar panels) and Under-Panel (UP – at a vertical projected point below a solar panel). In the dynamic AV plots (DAV), the instrumentation was installed in the same maize row in a way to be placed in the two different positions IP and UP. The tracking control in DAV plots permits to modify the tilt angle between – 50–50° on the E-W direction to follow the sun curse during the day-time and in a horizontal position during night-time.

R-squared. To provide an additional angle of analysis, we "extrapolated" this concept to analyze the radiation associated to the appearance of "one more leaf", by introducing the *PHY-r* (MJ/leaf), computed as *PHY* but using “radiative time” (accumulated daily *Rg-tot*) instead of *GDD*.

2.5. Gas exchange measurements

Plant gas exchanges (stomatal conductance and photosynthesis) have been measured for different sunny days with clear sky conditions whenever possible during the 2021 season with a TARGAS-1 Portable Photosynthesis System (PP Systems), to identify the impacts of Photosynthetic Active Radiation variations (*PAR*) on Stomatal Conductance (*gs*) and on the Net Photosynthesis Assimilation Rate (*A*). The apparatus was mounted to pinch a leaf horizontally, taking care to avoid shadows from the plot or other plants. Measurements started early in the morning and ended in the afternoon.

3. Results

3.1. Impact of the solar panels on agrometeorological variables

Fig. 3 shows the total amounts of the key agrometeorological variables measured in the different shading conditions. We preferred to show thermal time instead air temperature because is a more relevant (empirical) driver of crop growth and is mostly used in maize studies. Water inputs consider rainfall and irrigation. In Figs. 4–6, we focus our study on radiation and air temperature reductions Under-Panels, which are the two expected and documented variables affected in AV systems and that impact crop development in many ways. Relative humidity and wind were excluded from our analysis because of their marginal variations between the AV devices of Lavalette (Marrou et al., 2013a), and their secondary role in crop development.

In Fig. 3, the total solar radiation measured under the panels in the different AV plots led to shading rates of 29–38% in DAV, 30–35% in AVhalf and 54–56% in AVfull, depending on the season. These measured

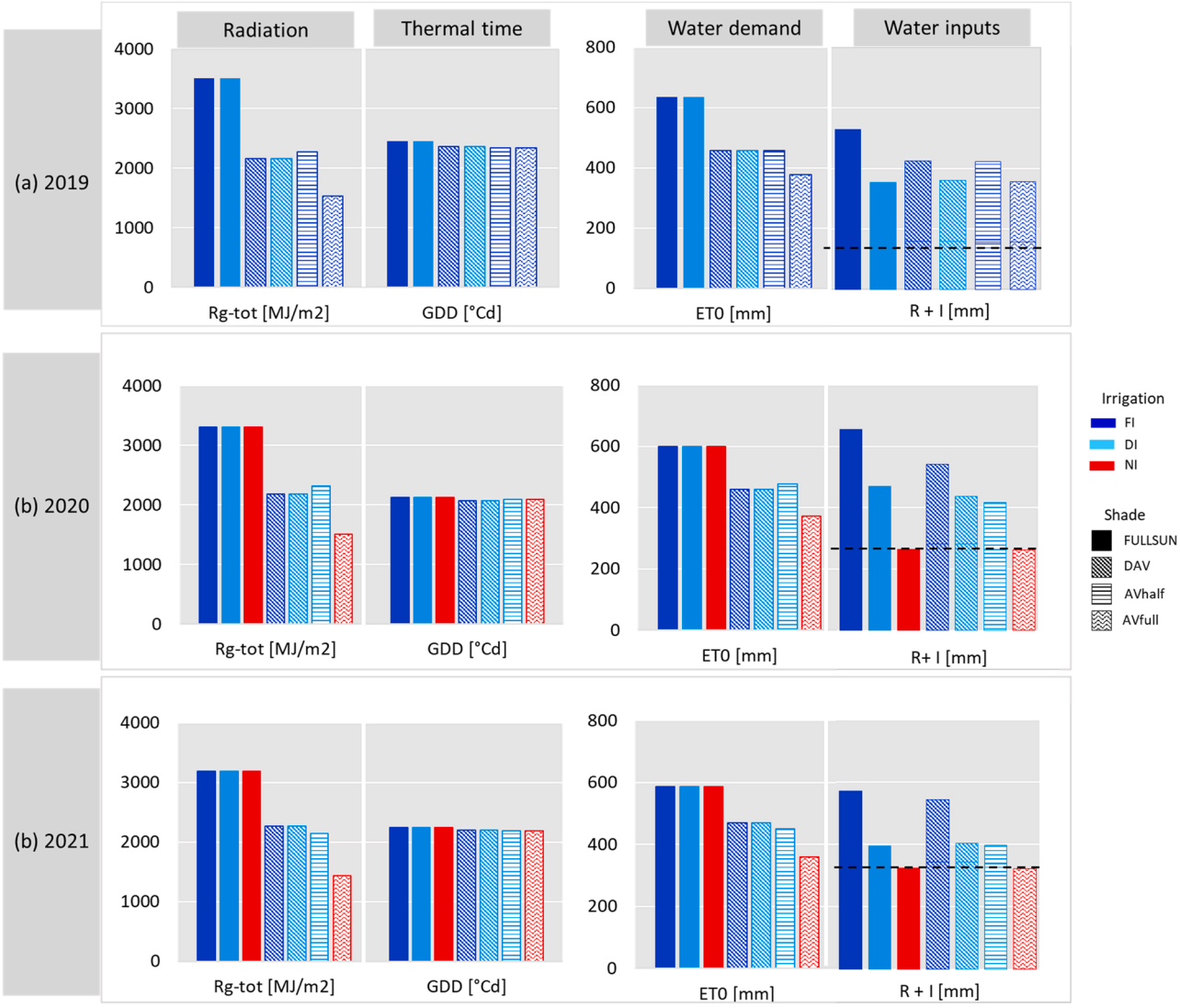

Fig. 3. Cumulated key agrometeorological variables measured from sowing until harvest during the three cropping seasons (a) 2019, (b) 2020 and (c) 2021: Total Global Radiation (*Rg-tot*) transmitted to the canopy (at 2 m) in AV plots, computed as the average of the IP and UP sensors; Growing Degree Days (*GDD*); Reference Evapotranspiration (*ETo*), considered as the climatic demand of water and was computed by the Penman-Monteith method for each radiative condition; Rainfall (*R*) and Irrigation (*I*) inputs. The colors represent the different irrigation treatments: dark-blue for Fully Irrigated (FI), light-blue for Deficit Irrigated (DI), and red for Not Irrigated (NI). Rainfall amount is represented by the horizontal dotted line colored in black in the R+I columns. Shade treatments are differentiated by the fill patterns of the columns: FULLSUN plots are represented by solid-filled columns, DAV by diagonal-lines filled columns, AVhalf by horizontal-lines filled columns and AVfull by zigzag-lines filled columns.

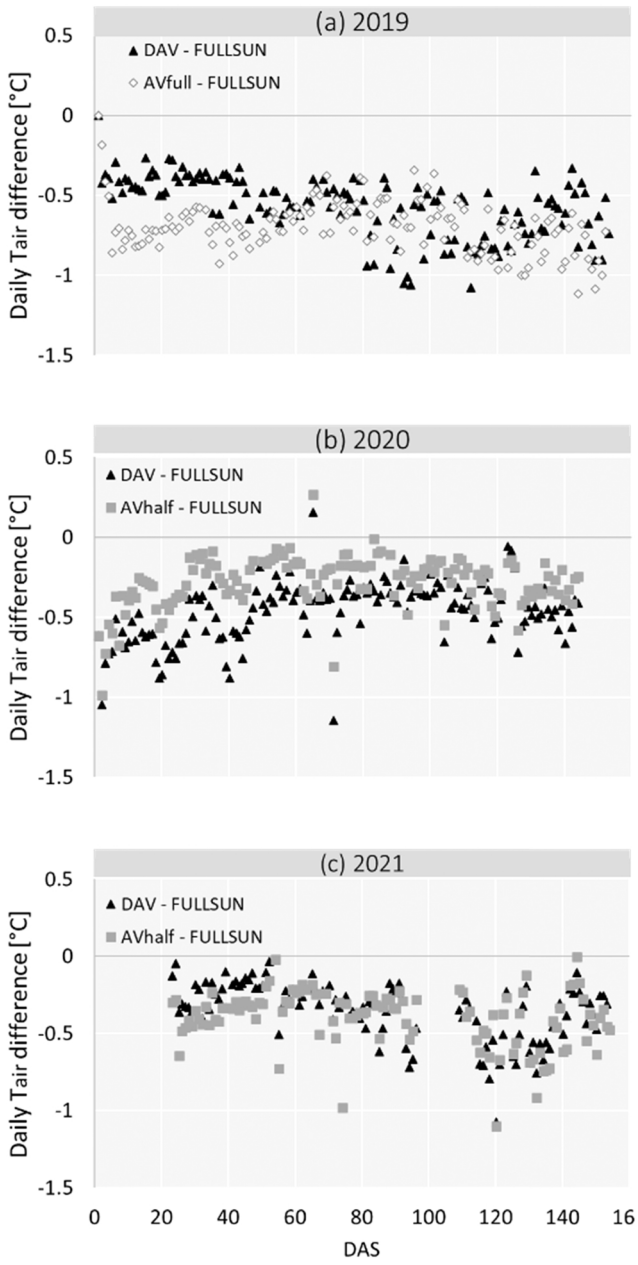

Fig. 4. Differences in the daily means of air temperature (T_{air}) between AV and FULLSUN plots for 2019 (a), 2020 (b) and 2021 (c). In 2019 the two monitored AV plots were DAV (west) and AVfull, while in 2020 and 2021 the two monitored AV plots were DAV (west) and AVhalf).

rates are consistent with those obtained previously in the same plots (Valle et al., 2017). The cumulated thermal time (cumulated *GDD*) did not vary significantly within the treatments, mainly because of the slight differences observed in air temperature (Fig. 4). As expected, the reference evapotranspiration reductions in AV were proportional to shading rates. The analysis of total water input (rainfall plus irrigation) shows that fully irrigated plots reached in general the reference evapotranspiration (except for FULLSUN in 2019). In deficit irrigated plots, the water inputs were in general lower than *ETo*, by 21–44% in FULLSUN, by 6–23% in DAV and by 9–10% in AVhalf. In FULLSUN not irrigated plot water inputs were 51–53% lower than *ETo*, however in AVfull, these values were only 6–17%. This is not surprising since radiation is the first driver of *ETo* equation. However, these results partly describe the effect of panels on the water budget, showing their impact on reduced reference evapotranspiration. The solar panels could affect the wind speed in each plot differently in a minimal way (see Marrou et al., 2013a), which represents a limitation on the usefulness of the calculated *ETo* values. The study of the impacts of solar panels on water budget will be delved in Section 3.2 thanks to soil water depletion analysis. A more detailed analysis based on the water budget (including actual evapotranspiration) was not included, given the uncertainties on different terms and due to spatial variability.

To analyze the intraday and daily dynamic patterns of incident radiation and air temperature, we focus on the 2019 cropping season because this year the monitored plots had more similar hydric conditions (reducing the risk of the influence of latent heat in air temperature measurements). Fig. 4 shows that the daily means of air temperature were only slightly affected by the presence of panels for the three years of experiments, with temperature reductions Under-Panels in the range of 0 to − 1.5 °C. However, when considering hourly temperature means, obtained from values taken each 10 min, the differences between the AV plots and the FULLSUN plot were wider, ranging between − 5 and + 3 °C. In other words, higher differences only exist in the intraday air temperature values, with possible short-term effects on crop health. Air temperature reductions in AV plots occurred mainly during the nighttime and then around (the solar) midday (Fig. 6a). On the other hand, air temperature augmentations in AV plots were observed in the afternoon (around 17:00), probably caused by air speed depletion around this time of the day. The slight reductions in daily air temperature registered in AV compared to FULLSUN also imply slightly reductions in daily *GDD*: between 0.0° and 0.5°Cd in DAV and between 0.0° and 1.2°Cd in AVfull, resulting in a seasonal reduction in cumulated *GDD* of 89 and 110 °Cd, respectively (Fig. 6b).

The spatial patterns of the available radiation under the AV plots of Lavalette have been modelled by Valle (2017) who showed more homogeneous spatial distributions of cumulated radiation in DAV plots when compared to AVhalf and AVfull plots. Confirmation is found in our experimental results: as an example, the daily cumulated radiation measured in DAV for the inter-panel (IP, 19.2 MJ/m^2) and under-panel (UP, 18.7 MJ/m^2) positions are very close on the sunny day of May 6, 2019 (Fig. 5a). with 19.18 and 18.71 MJ/m^2, respectively. However, we observed that their hourly dynamics displayed a “mirror” behavior (curves in phase opposition), with magnitudes controlled by a bell-shaped curve in the course of any given sunny day in the FULLSUN conditions. The temporal pattern was more irregular in the AVhalf (Fig. 5b) and AVfull plots (Fig. 5c) with far different cumulative daily radiation (Fig. 6a) between IP and UP positions. This difference in cumulative radiation amounts also exists when considering seasonal time scales (Fig. 6b). At the seasonal scale, the heterogeneity observed between the IP and UP positions for the AVhalf plot was high: the (cumulated) radiation measured at IP was around 65% of the UP radiation, whereas the UP radiation was around 93% of the IP radiation for the DAV plots. In the AVfull plot, the difference between radiations in the IP and UP positions was smaller than in AVhalf (IP radiation was 83% of UP), probably due to the homogenous shade observed in both positions before midday (Fig. 5c).

3.2. Soil water potential dynamics

Soil water potential is an indicator of soil water content, the evolution of which depends on evapotranspiration. As an illustration, we present the data collected during season 2020, where rain is less frequent. During that year, we also had the largest number of combinations of shading and irrigation levels (see Table 1). Fig. 7 shows the dynamics of soil water potential (*SWP*) observed from DAS 65 to DAS 145, covering the whole irrigation period, of the 2020 cropping season. For clarity, we chose to use the average between SWP values measured at 30, 60 and 90 cm depths, which we roughly considered as a proxy of the effort to be made by plant roots for water uptake from the soil. The first irrigation was applied on DAS 61, putting all irrigated plots (Fig. 7a, b, d, e, g) in water comfort conditions at the start of the measurements.

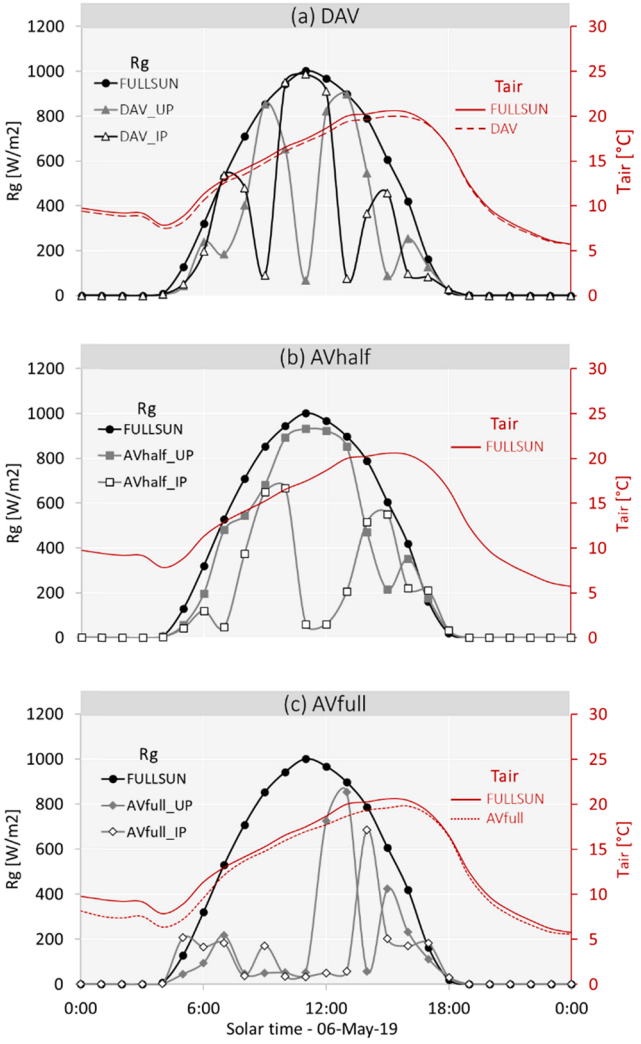

Fig. 5. Hourly dynamics of the incident global radiation (Rg) and air temperature for the DAV (a), AVhalf (b) and AVfull (c) devices, in comparison with FULLSUN conditions, showing differences between the IP (inter panel) and UP (Under-Panel) positions, for the sunny spring day of May 6th, 2019 (Tair was not measured in AVhalf for 2019). For legibility, the curves corresponding to air temperature data are in red, and the curves corresponding to radiation data are in black.

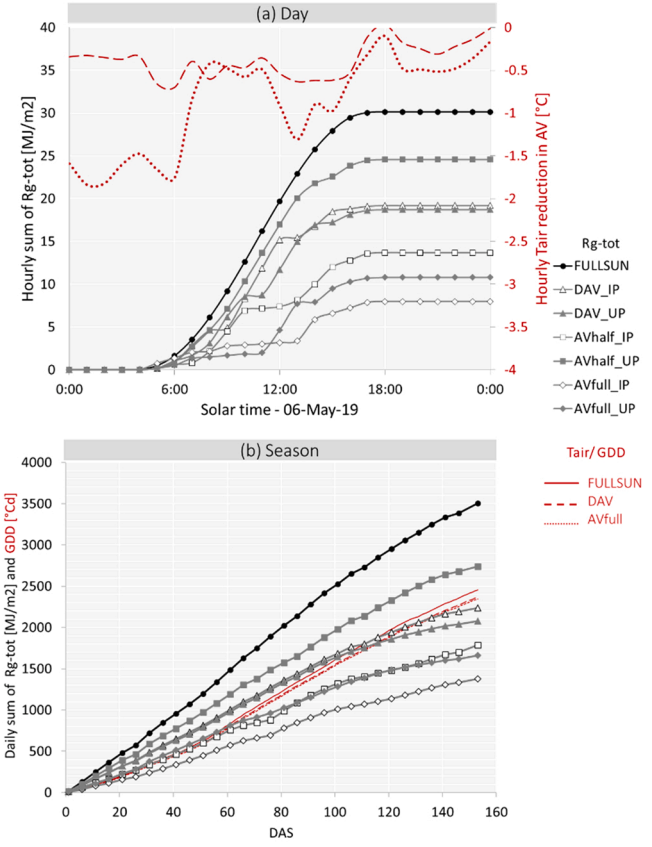

Fig. 6. Cumulative total global radiation (*Rg-tot*) for the FULLSUN, DAV, AVhalf and AVfull plots, also showing the difference between the IP and UP positions, and the hourly T_{air} reductions in AV compared to FULLSUN for the same spring day (a). Cumulative global radiation for the FULLSUN, DAV, AVhalf and AVfull plots, also shows the difference between the IP and UP positions, and the values of growing degrees-days (*GDD*) for the whole 2019 season (b). For legibility, the curves corresponding to air temperature data are in red, and the curves corresponding to radiation data are in black.

For the particular case of non-irrigated plots, *SWP* monitoring started later (on DAS 85) showing moderate to severe water stress over the whole monitored period and slightly conservation of soil moisture in AVfull (Fig. 7c) compared to the FULLSUN conditions (Fig. 7f), leading to a greener appearance of the plants in the AVfull plot.

The main general trends that we can draw from *SWP* dynamics are that (i) soil drying was slower in the shaded plots when compared to the FULLSUN plots, resulting in better soil water conservation and thus, reducing irrigation needs in AV and that (ii) soil drying dynamics and magnitudes were different between the IP and UP positions under the fixed AV device (AVhalf – Fig. 7b) when compared to the dynamic AV device (DAV – Fig. 7a, d), highlighting the advantage of using tracking systems to achieve a more regular soil water content in the plot surface. Going a bit more into detail, we observe that soil drying in the IP position of the AVhalf plot was slower when compared to the UP position (Fig. 7b) as the UP position receives more radiation (Fig. 7d), resulting in mild-moderate water stress in the UP position (*SWP* between −80 and −150 kPa) for most of the irrigation period, while soil water content was maintained high enough to hold *SWP* under the − 80 kPa stress limit. A limitation of our results was the absence of rain redistribution and runoff water measurements during rainfall events.

3.3. Phenology and vegetative growth

Table 2 shows the days after sowing (DAS) to reach emergence (VE), tasseling (VT) and silking (R1) phenological growth stages for the seven treatments, during the 2020 and 2021 seasons. We observed two general trends, (i) a delay for all shaded plots compared to the FULLSUN conditions (whatever the irrigation treatment) in the emergence and flowering stages (of 5–11 days, depending on the shading rate), and (ii) in all cases when combining moderate water stress and a moderate shade (DAV_DI and AVhalf_DI plots), the delay was larger than in fully irrigated or FULLSUN conditions.

In both 2020 and 2021 seasons, the delays were 5–7 days for emergence in the moderate shade treatments (DAV and AVhalf, shading rate of around 30–35%) and about 10 days in the high shade (AVfull, shading rate of around 50%). The delays in VT and R1 reproductive stages were different depending on the irrigation conditions in the moderate shade compared to FULLSUN: 4–7 days for VT and 4–11 days for R1 moderate shade fully irrigated plots; while in deficit irrigated plots, this delay was of 4–5 days and 3–5 days, respectively. Additionally, no difference was observed between DAV and AVhalf (except for R1 in 2021). The effect of irrigation conditions was also observed in the FULLSUN conditions, where the time needed to reach the VT stage varied with the irrigation treatment, being slightly longer (2–4 days) for deficit irrigated than for fully irrigated conditions. This analysis does not

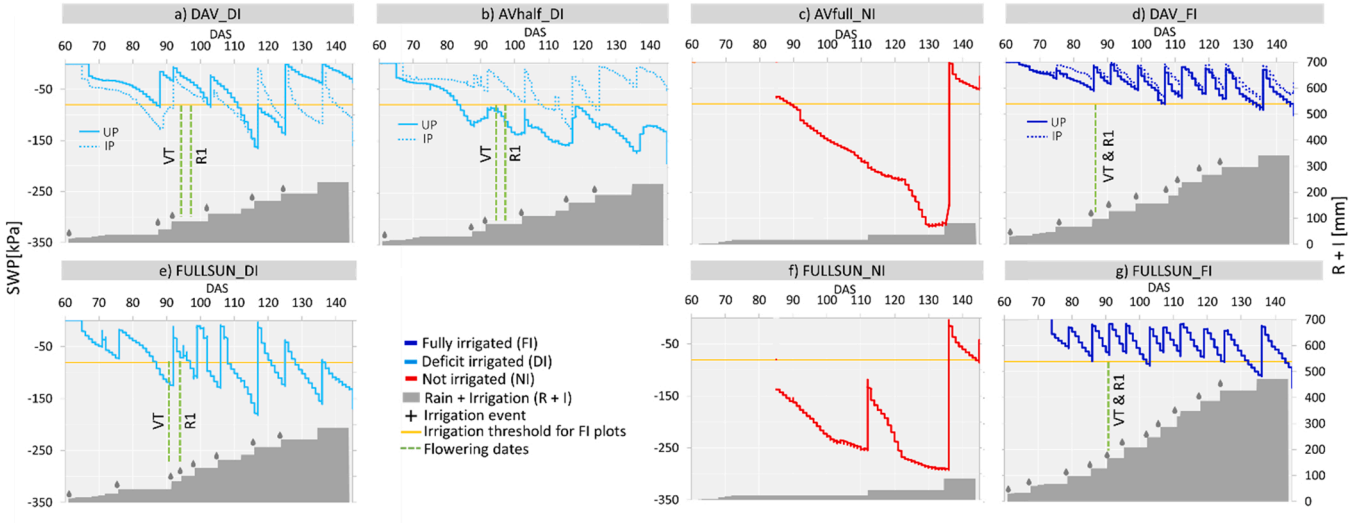

Fig. 7. Dynamics of Soil Water Potential (SWP) and cumulative Rainfall and Irrigation amounts (R + I) for the different combinations of shading (FULLSUN, DAV, AVhalf and AVfull) and irrigation (FI – Fully Irrigated, DI – Deficit Irrigation, NI – Not Irrigated) conditions, for the 2020 cropping season. The SWP values shown are averages of the values measured at 30, 60 and 90 cm depths, to be compared to the comfort threshold of − 80 kPa. The cumulative R + I course appears as grey areas at the bottom of each sketch, with values read on the right axis, while irrigations are depicted by grey drop symbols. The vertical dotted lines (in green) indicate flowering dates (VT and R1). On the (a), (b), (c) and (d) sketches, the SWP values provided by the Inter-Panels (IP) sensors are plotted as dotted lines while those provided by Under-Panel (UP) sensors are plotted as solid lines. For easier reading, the sketches are organized as in Fig. 1.

Table 2
Days After Sowing (DAS) to reach emergence (VE), tasseling (VT), and silking (R1) crop stages for the seven treatments during the 2020 and 2021 seasons. The "not reached" indication means that less than 50% of plants had flowered. The symbols in the stress column indicate the level of stress (moderate shade = •, high shade = ••; deficit irrigated = ┼, not irrigated = ┼┼). Not all the stress combinations showed in Table 1 were studied in 2020 and 2021 seasons.

Shade	Irrigation	Stress	2020			2021		
			VE	VT	R1	VE	VT	R1
FULLSUN	FI	Control (no stress)	12	87	87	11	87	87
FULLSUN	DI	┼	12	91	95	11	89	89
FULLSUN	NI	┼┼	12	Not reached	Not reached	11	Not reached	Not reached
DAV	FI	•	17	91	91	18	94	94
DAV	DI	•┼	17	95	98	18	94	98
AVhalf	DI	•┼	17	95	98	18	94	99
AVfull	NI	••┼┼	22	Not reached	Not reached	21	Not reached	Not reached

hold for NI conditions, neither reaching the VT nor the R1 stages during the two years of monitoring, whatever the shade level.

Concerning vegetative development, Fig. 8 shows the *GDD* and *Rg-tot* needed to develop a new leaf during the 2021 cropping season (the only season with leaf number monitoring). The main interpretations of Fig. 8 are: (i) as expected, the cumulated thermal time (*GDD*) and radiation (*Rg-tot*) variables were well associated with the leaf number, as the analyses have been conducted separately; (ii) the slope of the lines (phyllochron) for AV were lower than those in FULLSUN conditions, indicating that leaves in shade appear slower than in FULLSUN conditions and (iii) the key determinant for the number of leaves appears to be the shading or non-shading conditions while the irrigation strategy plays a limiting, cut-off role, as non-irrigated treatments prevented full crop development. The final number of leaves was optimal in the irrigated FULLSUN plots (15–16 leaves for the FI or DI treatments), while in the shaded AV plots the maximum number of leaves was limited to 12.

The effect of panels on the phyllochron (*PHY*) was clear (Fig. 8a): in the non-limiting light conditions (FULLSUN), the *PHY* value was 64 °Cd/leaf, while in the AV plots the *PHY* values increased with increasing shading rate: 79 and 81 °Cd/leaf in the DAV and AVhalf plots respectively (moderate-level shade) and 95 °Cd/leaf in the AVfull plot (high-level shade). These results are consistent with those of Birch et al. (1998) who reported increased phyllochron values with reduced irradiance. The *PHY* value reported in not-limited conditions (FULLSUN_FI) is not

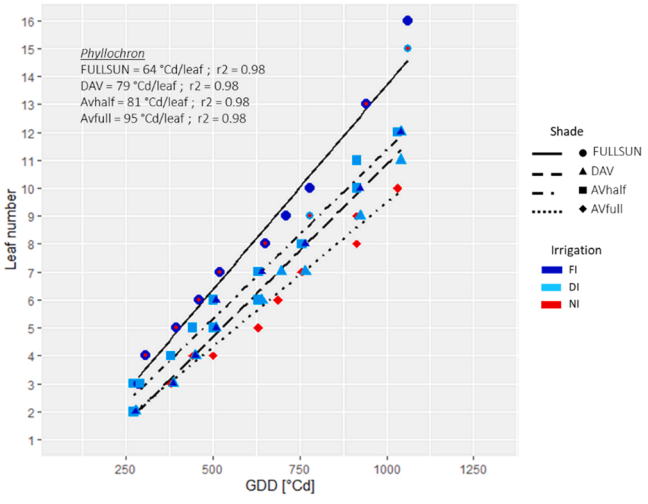

Fig. 8. Leaf number associated with cumulated Growing Degree Days (*GDD*) in 2021, for the different shading conditions: FULLSUN (circles and solid lines), DAV (triangles and dashed lines), AVhalf (squares and dot-dash lines), and AVfull (diamonds and dotted lines); crossed with irrigation strategies: Fully Irrigated (FI, in dark blue), Deficit Irrigated (DI, in light blue) and Not Irrigated (NI, in red).

far from the values reported by Verheul et al. (1996) among different maize cultivars (between 38° and 52°Cd/leaf). The irrigation strategy had no effect on *PHY* values (analysis not shown).

Consistently, Leaf Area Index (LAI) evolution largely depends on both radiative and hydric conditions, as shown in Fig. 9 with the maximum values of *LAI* (Leaf Area Index) for all experimental conditions (2019–2021), and the seasonal variation of *LAI* during year 2020 (the most complete data). As expected, the maximal *LAI* (*LAImax*) values decrease when less radiation is present and (or) when water is limited during the course of the season (Fig. 9a-c), the latter also affecting the shape of the *LAI* curve (Fig. 9d). As an example, in the presence of pronounced water stress (red curves), the *LAI* curve was lower for high shading rates (AVfull) than for FULLSUN conditions, suggesting that the presence of panels is not sufficient to compensate the effect of water deficit. In coherence, similar dynamics are observed in AV plots with similar shading rates (DAV, AVhalf) and similar irrigation amounts, suggesting that the dynamic rotation of panels in DAV had no significant effect on *LAI* dynamics. Finally, similar *LAI* dynamics were observed for moderate shading rates (DAV_FI) or moderate water deficit (FULLSUN_DI) which seems an interesting result for modelling purposes, suggesting introducing an overall stress indicator affecting the evolution of LAI.

3.4. Stomatal responses to shade

Fig. 10 depicts the typical dynamics of measured Photosynthetically Active Radiation (*PAR*), Leaf Temperature (T_{leaf}), Net Assimilation Rate (*A*), and Stomatal Conductance (*gs*) of maize leaves, in different conditions: FULLSUN fully irrigated (Fig. 10a), DAV fully irrigated in the two UP and IP positions (Fig. 10b and d) and DAV deficit irrigated only in IP position (Fig. 10c) that can be compared to Fig. 10d. In non-limiting conditions (Fig. 10a), we observe that the values of all measured variables increased from the beginning of the measurements to reach a maximum near midday, before a gradual decrease takes place to the end of the day, while in AV plots we observe the same trends but with the shading breaks, from a few minutes to few hours, in all processes measured. More specifically, the dynamics of *A* and *gs* were highly correlated to those of *PAR*, in shaded or FULLSUN conditions, for fully irrigated or deficit irrigation conditions and whatever the plant position to the panels (IP or UP). The effects of panels can also be observed on T_{leaf}, but the changes were less pronounced.

Furthermore, the experimental data show that plant reaction to *PAR* changes is neither immediate nor unique. During brief shadings, the stomata had insufficient time to adapt to *PAR* variations (see Fig. 11, which is a close-up of Fig. 10d) while in the case of prolonged shading the time needed to adapt was ca. 10 min. Fig. 11 shows that our data is coherent with those shown by Pearcy et al. (1997), indicating that responses of photosynthesis to increases in irradiance are not instantaneous and with the study of Meidner and Mansfield (1965) who showed evidence that the processes of stomatal opening and closing are different in nature, and that one is not simply a reversal of the other.

3.5. Crop production

Total Dry Matter (*TDM*) and Dry Grain Yield (*GY*) are provided in Fig. 12 for the three seasons. The main observations of this figure are: (i) as for the *LAI* values, both *TDM* and *GY* were reduced when irrigation and (or) radiation were reduced, thus in comparison with the FULLSUN and fully irrigated conditions (Fig. 12a). (ii) Moderate shading rates in DAV (−35%) and AVhalf (−30%) under fully irrigated conditions (Fig. 12b-c) reduced irrigation amounts by 19–35%, while for higher shading rates (AVfull, Fig. 12d) irrigation was reduced by 47%. (iii) Moderate shading rates in DAV and AVhalf under fully irrigated conditions produced similar *TDM* and *GY* compared to FULLSUN in deficit irrigation. (iv) When combining moderate water and radiation stresses (DAV and AVhalf in deficit irrigated conditions) the reductions in *TDM* were 40–53% and 22–51% in *GY*, indicating lower reductions in *GY* compared to *TDM*. (v) Finally, not irrigated treatments (whatever the shade level) produces higher *TDM* and *GY* reduction, between 71% and 80% and 66–83%, respectively, supporting the cut-off effect on crop development of high-water stress also shown in Section 2.3.

Table 3 gathers the final indicators for the water budget and crop production, for the different plots and treatments. Water Productivity of Irrigation (*WPI*) was higher in shaded plots under fully irrigated

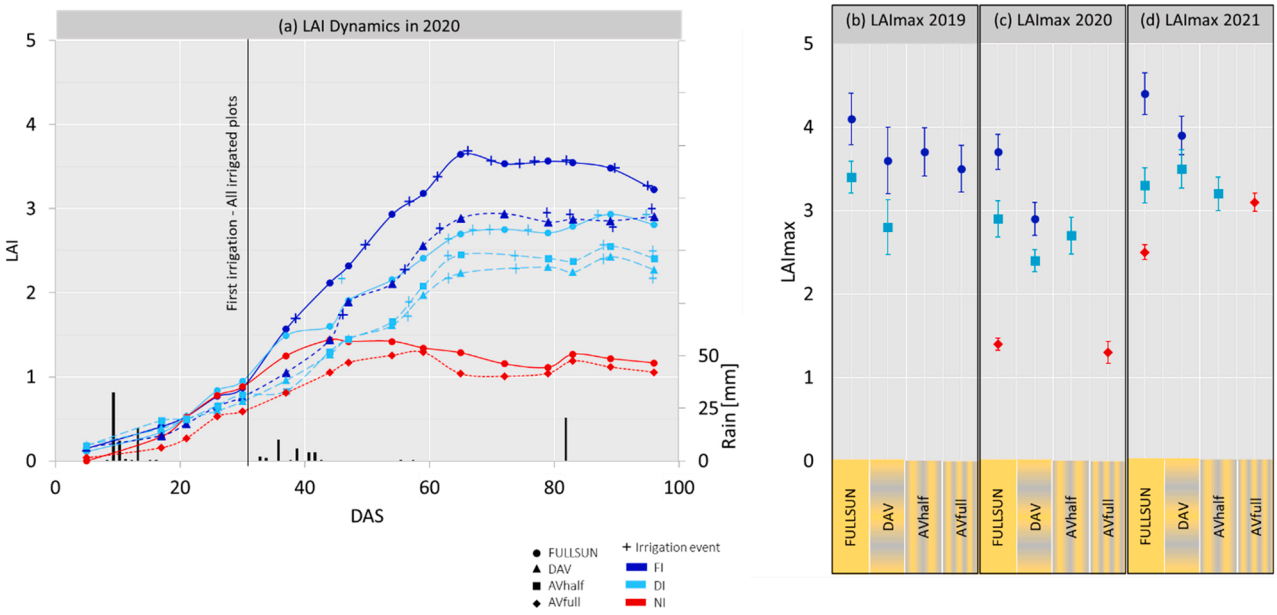

Fig. 9. Leaf Area Index (*LAI*) dynamic curves for the 2020 cropping season (a) and maximum values of LAI (*LAImax*) for the three cropping seasons, 2019 (b), 2020 (c) and 2021 (d), for the different combinations of shading (FULLSUN in circles, DAV in triangles, AVhalf in squares and AVfull in diamonds) crossed with irrigation strategies (FI – Fully Irrigated, in dark blue, DI – Deficit Irrigation, in light blue, NI – Not Irrigated, in red). In the sketch (a) the continuous lines represent the FULLSUN plots and dotted lines the shaded treatments, the crosses indicate irrigation events (in general, 40 mm for FULLSUN and 30 mm for DAV and AVhalf), and the histograms indicate rain amounts, read on the right axis. In sketches (b), (c) and (d), points indicate average values ± standard error.

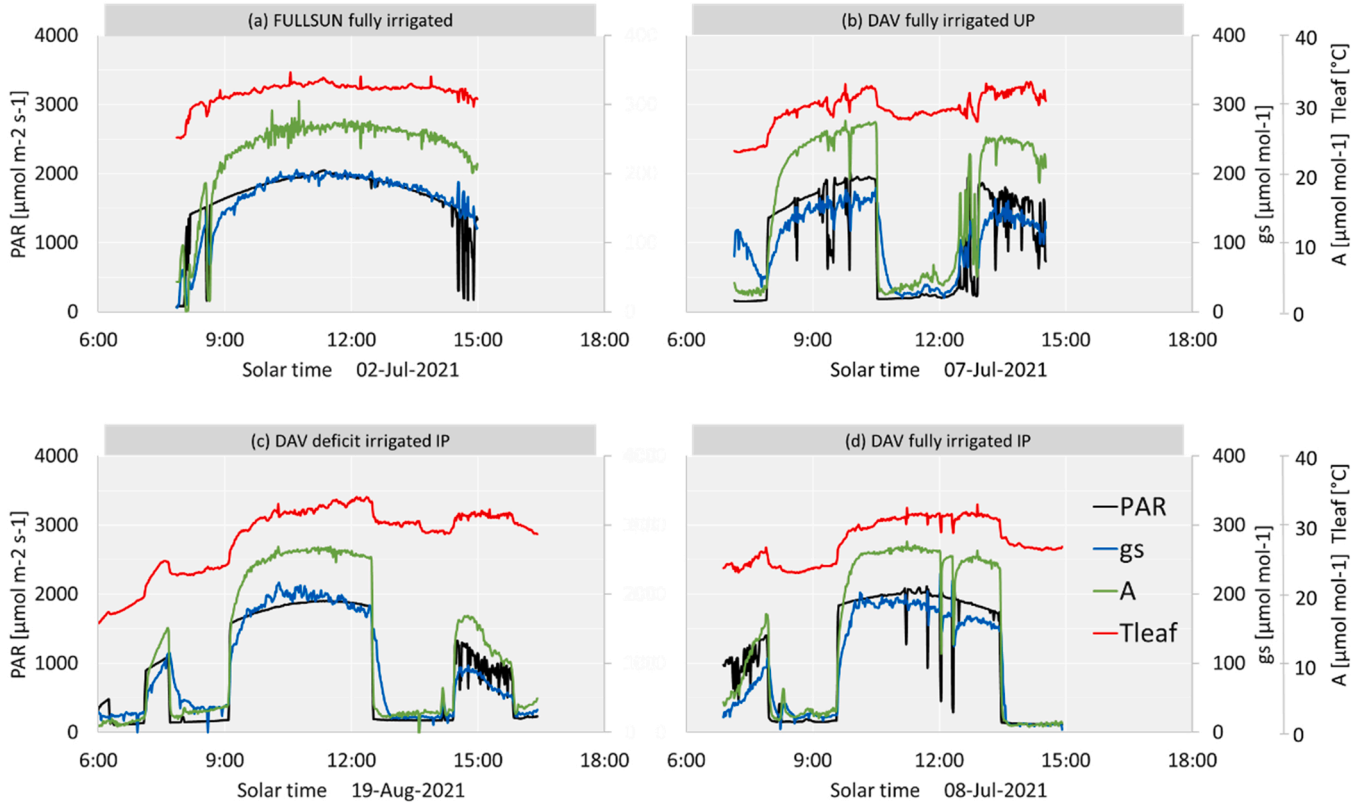

Fig. 10. Diurnal dynamics (6:00–18:00) of photosynthetically active radiation (*PAR*, in black), stomatal conductance (*gs*, in blue), net assimilation rate (*A*, in green), and leaf temperature (T_{leaf}, in red) measured on maize leaves by a Portable Photosynthesis System (1-minute timestep) in different clear-sky conditions during the 2021 cropping season: (a) FULLSUN fully irrigated, (b) DAV fully irrigated (UP position), (c) DAV deficit irrigated (IP position) and (d) DAV fully irrigated (IP position). The date of measurement is indicated at the bottom of the sketches.

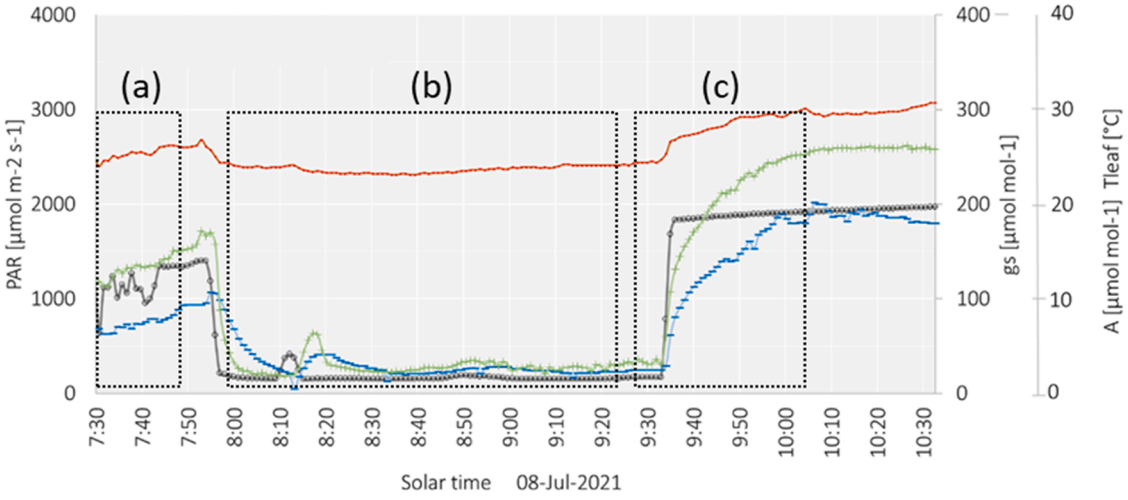

Fig. 11. Close-up on Fig. 10d, seeking the effects of brief shading (a), prolonged shading (b) and a sharp increase in incoming radiation (c). See the legend of Fig. 10.

conditions, especially in deficit irrigated plots. However, in terms of Water Productivity (*WP*), which also consider the rainfall inputs, we observe the inverse trend. Finally, the values of the Harvest Index (*HI*) varied between 0.48 and 0.57 in fully irrigated plots, between 0.47 and 0.67 and between 0.45 and 0.6 in not irrigated plots. Additionally, HI did not seem to be impacted neither by shade. The values of the *HI* varied between 0.48 and 0.6 in FULLSUN plots, between 0.47 and 0.67 in DAV and AVhalf (moderate shade) and between 0.45 and 0.52 in AVfull (high shade). These values correspond to values reported in maize (0.20–0.56) for different growing conditions (Ion et al., 2015). However, our estimations were based only in aerial *TDM* without considering the underground biomass (root system was not harvested). Taking into account root mass in the estimations should decrease *HI* in all plots.

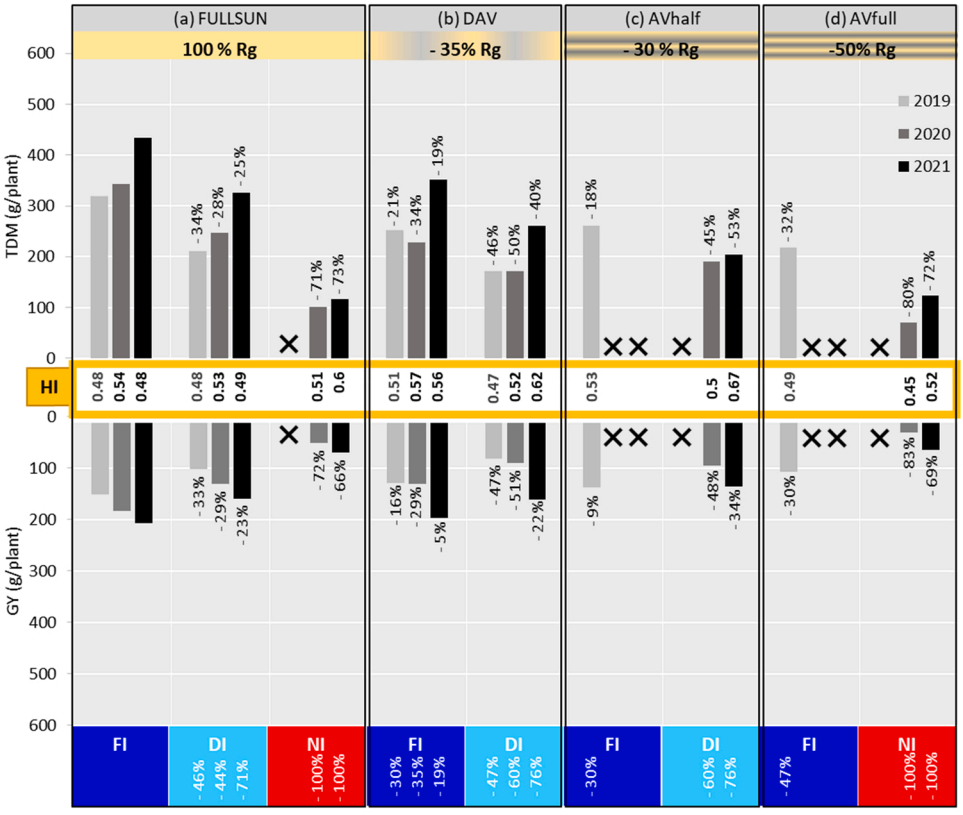

Fig. 12. At the top, Total Dry Matter (*TDM*), and at the bottom Dry Grain Yield (*GY*) for the (a) FULLSUN, (b) DAV, (c) AVhalf, and (d) AVfull plots, for the three cropping seasons (2019, in light-grey; 2020 in dark-grey and 2021 in black). The three irrigation strategies (FI – Fully Irrigated, DI – Deficit Irrigated, and NI – Not Irrigated) conditions. The percentages over the histograms indicate the relative reduction compared to the FULLSUN fully irrigated plot, in the same year. Harvest Index (HI) is indicated in the middle of the figure (the yellow square). The X symbol indicates that this combination of stress was not studied in the current season.

Table 3
Crop growth and production *indicators for 2019, 2020 and 2021 cropping seasons:* LAI_{max} *is the maximum value of* LAI *recorded from* L*AI-2200 C – LICOR measurements. Values of* LAI *allometric measurements realized at the end of the 2021 season are presented in parenthesis.* TDM *and* GY *are, respectively, the mean weight of total dry matter of aerial parts and dry grain yield of the ears from 40 plants sampled at each plot, and* HI *is the harvest index computed for each plot* (GY/TDM). WPI *is the Irrigation Water Productivity computed as* TDM *(in kg) divided by* I *(in* m^3*), considering a plant density of 8.3 plants by* m^2. WP *is the Water Productivity, with the same logic as* WPI *but using* R+I *in the denominator. For legibility, the P value is reported only for AV plots related to FULLSUN (under similar irrigation conditions). After* TDM *and* GY *variables, the same letter* (ns *columns) indicates no significant difference between means (Turkey HSD test,* $P < 0.05$).

Shade	Irrigation	LAI_{max}	TDM			GY			HI	WPI	WP
		[m^2/m^2]	[g/plant]	ns	P	[g/plant]	ns	P	[-]	[kg/m^3]	[kg/m^3]
2019											
FULLSUN	FI	4.1 ± 0.3	318.8 ± 104			151.9 ± 43	a		0.48	7	5
FULLSUN	DI	3.4 ± 0.2	210.2 ± 77	b		101.7 ± 41	b		0.48	8.5	4.9
DAV	FI	3.6 ± 0.4	252.2 ± 79	a	< 0.0001	128.3 ± 35	a	< 0.0001	0.51	7.9	5.1
DAV	DI	2.8 ± 0.3	172.0 ± 67		< 0.01	81.2 ± 39		< 0.001	0.47	7.2	4.1
AVhalf	FI	3.7 ± 0.3	260.9 ± 66	a	< 0.0001	138.4 ± 36	a	< 0.050	0.53	8.2	5.2
AVfull	FI	3.5 ± 0.3	217.0 ± 51	b	< 0.0001	106.7 ± 29	b	< 0.0001	0.49	9	5.2
2020											
FULLSUN	FI	3.7 ± 0.2	343.1 ± 86			183.9 ± 33			0.54	7.3	4.4
FULLSUN	DI	2.9 ± 0.2	246.9 ± 84	a		130.7 ± 40	a		0.53	10	4.4
FULLSUN	NI	1.4 ± 0.1	107.6 ± 35	c		51.8 ± 35	c		0.51	—	3.2
DAV	FI	2.9 ± 0.2	227.9 ± 48	a	< 0.0001	130.2 ± 31	a	< 0.0001	0.57	7.3	3.6
DAV	DI	2.4 ± 0.1	193.0 ± 63	b	< 0.0001	89.4 ± 34	b	< 0.0001	0.52	9.3	3.4
AVhalf	DI	2.7 ± 0.2	190.0 ± 41	b	< 0.0001	95.5 ± 32	b	< 0.0001	0.5	10.2	3.8
AVfull	NI	1.3 ± 0.1	69.3 ± 30	c	0.157	31.4 ± 26	c	0.430	0.45	—	2.2
2021											
FULLSUN	FI	4.5 ± 0.1	434.2 ± 73			206.9 ± 30	a		0.48	14.6	6.3
FULLSUN	DI	4.1 ± 0.1	326.5 ± 99	b		160.0 ± 44	b		0.49	38.3	6.9
FULLSUN	NI	2.4 ± 0.2	116.6 ± 48	c		70.5 ± 22	c		0.6	—	3
DAV	FI	2.6 ± 0.1	352.1 ± 86	b	< 0.0001	196.3 ± 47	a	0.923	0.56	14.7	5.6
DAV	DI	2.2 ± 0.1	260.6 ± 53		< 0.01	161.2 ± 52	b	0.999	0.62	36.2	5.7
AVhalf	DI	2.4 ± 0.1	203.6 ± 61		< 0.0001	135.7 ± 38	b	0.147	0.67	28.3	4.4
AVfull	NI	1.7 ± 0.1	123.5 ± 41	c	0.999	64.0 ± 36	c	0.999	0.52	—	3.2

4. Discussion

4.1. Phenological and growth responses of maize to radiative and water stresses

4.1.1. Phenological delay

Plant emergence was delayed proportionally to shade intensity as shown in Table 2. Plant emergence in maize is mainly influenced by soil temperature among other factors (soil water content and seed depth). In our study, the only difference between plots during seeding was shading, causing a reduction in soil temperature, and directly impacting emergence time. Soil temperature reduction Under-Panels in the Agrivoltaic platform of Lavalette was not presented here but had already been reported by Marrou et al. (2013a-b) both in irrigated and not irrigated conditions. A reduction in soil temperature was also described under field AV conditions in Germany (Armstrong et al., 2016) and Italy (Amaducci et al., 2018), suggesting a generalized effect of shade-cooling soil temperature (at least, in temperate and Mediterranean conditions). The delay observed in flowering stages VT and R1 were maintained in a similar proportion to shade such as in emergence. The first hypothesis that could be derived from this fact is that the earlier delay in emergence may be the principal factor affecting the subsequent phenological development (leaf stages and flowering). In this sense, Earley et al. (1966) also reported flowering delay in maize under shading but when shade was applied during vegetative growth (avoiding the delay in emergence such as in our experiments). Thus, the delay in flowering was probably more related to leaf stages development, also affected by shade. Indeed, a reduced final number of leaves (Fig. 8), may explain the delay in VT and R1 stages, as the time elapsing to flowering from emergence is associated with the final number of leaves per plant (Tollenaar et al., 1979). Moreover, Birch et al. (1998) also reported similarly a reduction in the number of leaves under 55–73% level of shade.

The inhibition of flowering due to severe water stress was clear, but moderate stress (such as in deficit irrigated plots) seems not to affect VT. However, this can lead to a slight delay between VT and R1 (in shaded and in unshaded conditions), which was not observed in fully irrigated conditions. This effect was more evident in 2020, likely due to the drier conditions of the season. This delay between VT and R1 is related to the Anthesis—Silk Interval (ASI), one of the best indicators of how plants respond to stress (water, light, nutrients) during flowering. A similar response of maize was described by Nesmith and Ritchie (1992) under hydric deficit conditions. In our experiments, we did not observe a delay between VT and R1 under shade, suggesting that the presence of panels in AV does not influence ASI.

4.1.2. Vegetative development

In a more detailed analysis of vegetative development, one of our main findings is the influence of shade on phyllochron (Fig. 8). The emphasis is placed here on the fact that more temperature is needed for a new leaf formation when less radiation is available. Similar results were discussed by Birch et al. (1998) in both controlled atmosphere and field conditions. They reported that shading lengthened phyllochron causing an increase of 2–4 °Cd for each MJ decreased in daily *PAR*. Since leaf appearance (phyllochron^{-1}) is commonly linked only to thermal time, it was not expected that soil water or light influenced phyllochron. From our results, in the case of soil water, we can reaffirm that this factor (water) has not influence on phyllochron. The mentioned influence of shade on phyllochron led us to propose the relationship of leaf appearance to "radiation time" (cumulated *Rg-tot*) instead of thermal time (cumulated *GDD*) to compare both relationships separately (Supplementary Fig. S2). It was interesting to observe that leaf appearance showed a similar (linear) dependence on radiation such as with thermal time (Padilla and Otegui, 2005). This was probably due to the close relationship between radiation and air temperature and because leaves (and plant) temperature is also strongly affected by radiation. Moreover, when computing *PHY-r* (phyllochron using radiation instead of temperature) and distinguishing between data obtained in UP (under-panel) and IP (inter-panel) positions in AV plots, we observed differences in *PHY-r* values between the UP and IP in the fixed devices AVhalf and AVfull. These differences could be ignored (almost certainly) when using a classical thermal time relationship, because of the slight variations in air temperatures recorded Under-Panels compared to FULLSUN (see Figs. 5–6). This last statement suggests that one could use *PHY-r* instead of *PHY* in systems with strong spatial heterogeneities in radiation. This may open new pathways to define the determinants and controls of crop development, especially for spatial-discrete crop modelling in AV systems (and probably also in agroforestry). Another way to improve phyllochron estimation in AV systems may be the use of plant (or leaf, steam or canopy) temperatures instead of air temperature, since this temperature is more impacted by the presence of panels (directly determined by energy balance) than the mean air temperature, as suggested by leaf temperature dynamics (see Fig. 10). We could not deepen this idea without monitoring of daily plant-based temperatures, but we suggest exploring it in further experiments or by modelling (i.e., Blonder and Michaletz, 2018) to improve carbon and water fluxes estimations. Therefore, models using thermal time could be enriched by including shade effects on phyllochron or energy balance to better aggregate the possible misrepresented physiological responses of the crops in AV.

The complementary analysis of vegetative growth using Leaf Area Index (*LAI*) dynamics (Fig. 9) and maximal values of *LAI* (*LAImax*) led us to affirm that water deficit and shade have more impact on individual leaf size than on leaf appearance, thus in total leaf area of the plant (and of the plot). This response is well-known and related to plant adaptive traits, most of them showing that water and carbon emerge as the main limiting factors of leaf expansion (Pantin et al., 2011), even if the literature remains controversial about their respective contributions to final leaf area. Some of the more cited responses to stress (water, shade, nutrients) at the leaf level are the reductions in leaf area, mass, and thickness (Givnish, 1988) and photosynthetic characteristics modifications (i.e., Ren et al., 2016).

Concerning the effects of the "Solar Tracking" panel rotation strategy implemented in DAV compared to AVhalf plots (having different intraday patterns but similar daily total irradiance as shown in Figs. 5–6) we did not observe a clear difference in *LAImax* values (Fig. 9) in fully irrigated conditions, neither in deficit irrigated conditions. This is in contrast with the inverse relationship between the optimal maximum photosynthetic capacity and the frequency of low to high light transitions reported by Retkute et al. (2015), who suggest that the effects of shade in leaf growth will depend also on the intraday patterns of shade. The effects of dynamic panels in leaf appearance were neither clearly affected in DAV compared to AVhalf in Fig. 8. These findings suggest that vegetative growth (i.e., leaf appearance and canopy size) at the plot scale were not strongly affected by the spatial heterogeneity of radiation transmission to the crop. To complement this analysis, specific allometric measurements of *LAI* in the UP and IP positions could be used to describe canopy growth heterogeneities, especially in fixed-AV installations characterized by high crop irradiance heterogeneity. Also, we encourage the general use of *LAI* to describe vegetative development in AV systems (i.e., for modelling purposes) since this index is a critical variable in processes such as photosynthesis and respiration and allows to capture the effects of both stresses analyzed here, when we do not require a "fine" spatial discretization of crop growth.

4.1.3. Crop production

Concerning the final agricultural production, we observed in Fig. 12 the negative effects of irradiance reduction and (or) water stress, as documented by several authors in different maize-shaded experiments (e.g., Mbewe and Hunter; Zhang et al., 2006; Yuan et al., 2021) and in other crops that are not-tolerant to shade grown in AV (Weselek et al., 2019). Particularly, our results differ from those reported by Amaducci et al. (2018), who reported higher average maize yield under AV

scenarios than under not shaded conditions when water was limiting (results from simulations performed with climate data from 37 years). This shows the limitations of current formalisms used in crop models to simulate yield production. The reduction of the maximal and final values of *LAI* combined with the higher phyllochron (lower leaf appearance rate) caused by the panels (Figs. 8–9) likely affect light interception and seem prone to explain the reported negative effects on the final *TDM* and *GY* values. Furthermore, yield production studies have shown that the effects of stress depend on the type, severity, and duration of the stress, as well as on the stage of development of the plant when the stress is applied, the reproductive stages (VT and R1) being the most detrimental to dry grain yield (Earley et al., 1967; Tollenaar, 1977). In particular, grain filling is said to be affected at the start of the critical period of grain set formation if solar radiation or (and) temperature sharply declines during this period (Otegui and Bonhomme, 1998) thus reducing the number of grains per grain set (Loomis and Connor, 1992). In all of our shaded plots, the shade was permanent, explaining the high yield reductions as documented by Ren et al. (2016), who also reported the lowest reduction of net photosynthetic rate when shade was applied only from the sixth leaf stage (V6) to silk (R1). In turn, Earley et al. (1966) showed that shading for 21 days during the reproductive phase was more detrimental to grain production per plant than shading for longer periods during vegetative and maturation phases. They also reported that a reduction of light from 100% to 70% essentially eliminated the development of the second ear, which was similar to that in our experiments.

Concerning the effects of water, in Fig. 7 we can observe that water depletion was high in the pre-flowering and flowering periods for deficit irrigated treatments, affecting crops during this sensitive period. In not irrigated maize plots (whatever the shading rate) the effect of water stress, particularly in 2020 (Fig. 12) was evident, confirming the sensitivity of maize to the erratic behavior of rains (Campos et al., 2004). We highlight the strong effect of water deficit in not irrigated plots on flowering failure (under shade or not), affecting crop production. However, the data shown in Fig. 12 for FULLSUN not irrigated plots correspond to "survival" plants in the plot, where most of them died, while in AVfull most of them were still green at harvest. In maize, grain filling shows a dependence on Anthesis—Silk Interval (ASI) and is particularly associated with a reduction in photosynthate formed during grain formation (Edmeades et al., 2000), probably impacting grain yield in deficit irrigated plots.

The smaller relative reduction of *GY* (in comparison with *TDM*) in the fully irrigated AV plots and some of the deficit irrigated plots shown in Section 3.5, can be explained by the photosynthetic acclimation process (Hirth et al., 2013) and possibly also by the internal mechanisms of maize plants to recycle the surplus of water during grain filling (Zhang et al., 2022). Photosynthetic acclimation is how plants alter their leaf composition and physiology over time to enhance photosynthetic efficiency, productivity, and allocation. We hypothesized that the maize plants adjust the light-response characteristics to balance the efficient use of absorbed energy in fluctuating light (varying in both intensity and frequency) to maximize daily carbon gain and to maintain a specific level of photosynthesis. This affects leaf growth but promotes at the same time a concentration of assimilates on grain formation, reducing the impact on *GY*. However, this hypothesis should be taken carefully, because in C4 plants, photosynthesis is less phenotypically "plastic" than C3 photosynthesis, and this may contribute to the more restricted adaptation to intermittent light (Sage and McKown, 2006). The water recycling mechanism of maize plants (by back-flows capacity via the pedicel phloem-xylem system connecting grain and cob) could allow the storage of the "surplus water" applied during water comfort periods (for example just after an irrigation event) in cob tissue, ensuring water availability for grain filling during slight or moderate water stress in deficit irrigated plots. Thus, complementary measurements of photosynthetic rates would be needed for the evaluation of this specific effect of shading considering the effect of growth stages and water status of the plant on the photosynthesis response of maize.

In 2021, we observed smaller reductions of *TDM* and *GY* in all cases, even when water irrigation reductions on deficit irrigation (DI) treatments were higher (71–76%) compared to 2019 and 2020 (44%−60%). This is because 2021 was a rainy year with significant rainfall events throughout the season (323.5 mm of cumulated rain during the crop season, compared to 264 mm and 149.5 mm during 2020 and 2019, respectively). This is confirmed by Fig. 7 in which we observe that water depletion was high around DAS 80–100 (pre-flowering and flowering period) in deficit irrigated plots in 2020. So, deficit irrigated plots were less stressed during vegetative, pre-flowering, and grain-filling stages in 2021, which are the most sensitive stages to stress (shade or limited water) as shown by several authors (e.g., Tollenaar, 1977). This resulted in higher production with fewer irrigations in 2021. However, grain yield production in stress conditions depends on the type, severity, and duration of the stress, as well as on the stage of development of the plant when the stress is applied (Mbewe and Hunter, 1986), highlighting the need for more trials with stress applied in different stages to complete the analysis.

4.1.4. Some considerations to interpret the results

It is important to note that the different shading patterns implemented for this experiment in the DAV plot represented only the so-called "Solar Tracking" strategy implemented in our experiments, which is a shading strategy devoted to maximizing light interception and not favoring crop production. In addition, the fixed AV devices studied here are not the only configurations that could be implemented, since a multitude of other possibilities exist in terms of panels' orientation, spacing, dimensions, height, and movements (degrees of freedom). Our experimental designs raise questions about the potential to generalize results because the shade applied could be different in other configurations, inducing different crop responses. Thus, further studies are necessary to evaluate different shading strategies, particularly in DAV devices, adapting the tracking panels strategy (and shading rate) to the different phenological stages, intending to minimize the effects of both stresses studied here.

Finally, we aimed to analyze and illustrate contrasted cases, and especially to evaluate the differences between dynamic and fixed plots to draw some preliminary conclusions, hopefully, useful and generic enough for future modelling aims. Additionally, it is still difficult to affirm that the crop responses shown here are specific to the light limitation in AV, since there are many adaptation traits in plants that vary in response to irradiance level and to other environmental factors, many of which are themselves correlated with irradiance level (Givnish, 1988). Furthermore, different maize genotypes may respond differently to shading (Yuan et al., 2021), adding a feature to minimize crop loss production in AV by shade-tolerant genotypes. Late sowing dates (as in the 2019 cropping season) may decrease the source/sink ratio in maize (Bonelli et al., 2016), which can also help to explain the lower yield in 2019 (Fig. 12).

4.2. Intermittent shading in AV as a way to manage water scarcity?

The shading patterns from the panels improved the water status on maize, reducing applied water in fully irrigated plots (Fig. 12), in a similar proportion compared with previous results in other crops studied under similar AV systems, such as lettuce (Elamri et al., 2018) and apple trees (Juillion et al., 2022). Higher Water Productivity of Irrigation (WPI) in deficit irrigated plots (shaded or not) compared with fully irrigated conditions shown in Table 3 supports previous data showing higher yields per unit of irrigation water applied in maize under regulated deficit strategies (Huang et al., 2011; Zou et al., 2021). Improved WPI in AV (in fully irrigated conditions) reported in Table 3 is probably related to the capacity of AV systems to (i) reduce reference evaporative demand (*ETo*) under shade (Fig. 3), and (ii) to slow down soil water depletion (Fig. 7), both reducing the actual evapotranspiration of any

crop (not measured directly in our study). It is also important highlight the fact that in AV systems, radiation reduction seems to be the first-order factor affecting *ETo* estimations, when comparing with reduced air temperature and reduced relative humidity under panels and to hypothetical wind speed reduced under panels of 30% (see supplementary Fig. S4).

An interesting fact that we observed in Fig. 7 is that in fixed AV systems (for example in the AVhalf plot on Fig. 7b), soil water conservation was strongly different depending on the UP (under-panel) or IP (inter-panel) positions when radiation distribution is heterogeneous. Indeed, in fixed devices the rain redistribution is always impacted by solar panels, with a high concentration of intercepted rain onto the soil at the lower edge of the solar arrays and much less runoff to the soil area under the panels, as showed by Elamri et al. (2018b) in the same experimental platform of our study. They also mentioned that this redistribution is, to some extent, attenuated within the soil due to lateral transfers at the soil surface (ponding), and within the soil profile where significant lateral dispersion coexists with gravity. This underlines the relevance and the potential benefits of tilting-angle panels (or other dynamic structures) to homogenize altogether (i) transmitted radiation (as showed in Fig. 6), (ii) rain redistribution (as demonstrated by Elamri et al., 2018b) and (iii) soil water depletion (as demonstrated in Fig. 7). This is probably related to reduced crop development and growth in IP areas (thus reducing root activity and reduced water uptake capacity). Root development and underground biomass were not measured in our experiments; however, it is well known that shading has a strong impact on the development of roots in the upper soil layer, significantly decreasing the root morphologic and activity indices (Gao et al., 2017). A similar effect on soil water conservation is observed in finely textured soils, by making soil water available at critical stages of maize development (Huang et al., 2011).

Hence, provided the radiative and water stresses are not too limiting, the use of predefined or real-time control algorithms of the panels is expected to be powerful enough to "force" a daily shading strategy throughout the crop season, able to fulfill several objectives: (i) reduce water application during the irrigation period, (ii) protect the crops during the hottest days of the season, or during water-sensitive periods of the crop, (iii) reduce yield losses in conditions requiring deficit irrigation strategies. Particularly in not irrigated or water-scarce contexts, operating the panels to permit soil drying at the seedling stage plus further mild soil drying at the stem-elongation stage, or applying deficit irrigation from V8 to maturity may be an optimum irrigation method to maximize maize production as reported by Kang et al. (2000) and Zou et al. (2021) in semi-arid conditions. Additionally, the delay observed in flowering (or those of the other phenological stages) may also be used to prevent or dampen the risk of water stress during the critical period for grain set around flowering (Hall et al., 1971), for example in an attempt to match flowering with rain forecasts, especially given the uncertainties in projected future rainfall and water allocations. This could be relevant in regions where rainfall mostly occurs in the early crop growth stages before the crop faces water stress from the pre-flowering to late grain-filling stages, declining crop production.

The seasonal-scale shading strategies could also be combined with shading strategies decided at much shorter temporal scales (throughout the day) to (i) reduce water depletion and daily evapotranspiration, (ii) protect the crop during the hottest period of the day to reduce crop stress or (ii) optimize diurnal photosynthesis until the saturation point is reached, i.e. maximize biomass production. The potential optimization of water use within agrivoltaics is expected to be substantial by improving the efficiency of water use at the plant level. However, in order to implement finer strategies of shadow control, it seems necessary to explore the factors controlling stomatal behavior, specifically irradiance and leaf water potential, as well as their interactions. In a preliminary attempt, a careful analysis of the comparisons in Fig. 10 leads to two key generalizations: (i) the stomatal behavior measured for maize leaves under different stresses (water and light) responds directly to radiation in all cases, and (ii) the responses seem proportional to radiation. In further research, this could give the possibility of real-time control, based only on radiation dynamics (considering shading periods) to target, simultaneously, water savings and reduction of productivity losses caused by radiation stress. However, this generalization must be taken carefully, because stomatal closure can appear before light reduction under moderate-severe water stress (Supplementary Fig. S3), making more complex the optimization in water deficit conditions.

Spatial heterogeneities make difficult the estimation of actual evapotranspiration through water budget. The presence of panels negatively influences rain redistribution uniformity, super-imposed with the spatial patterns due to irrigation application but with distinct spatial and temporal patterns. Models could be used to characterize these patterns (see e.g., Elamri et al., 2018b for rain distribution) but we recommend specific measurements to evaluate actual evapotranspiration, for instance with the use of lysimeters, and validate the water budget modelling under AV systems. As well, these results highlight the need to investigate the use of solar arrays for water harvesting with the aim to limit water run off to the plot perimeter and to redistribute this harvested water by uniform irrigation. A parallel study in AV systems targeted this subject (Chekired et al., 2022). Clearly, the possibility to orient solar panels opens a large diversity of optimization strategies of agrivoltaic structures, in terms of design and real-time operation, whether, for example, water use efficiency or economic yields are to be maximized.

4.3. *Perspectives for maize yield prediction in AV: towards time and spatial discretization?*

The global radiation transmitted to a specific point under the AV structure varies within the day, causing different dynamics depending on the configuration of the panels, and is mainly controlled by the density of modules and the chosen operation strategies (in dynamic devices). However, prediction tools (crop models, water balance, phenology chart) are mainly based on photoperiod and temperature values (Kiniry, Bonhomme, 1991). Ignoring intra-day variations by using daily-averaged values can lead to significant errors in terms of estimated light interception and carbon assimilation by crops, and then of crop development, as shown by Chopard (2021).

The results presented here for maize in different intermittent shadow patterns reveal the importance of space discretization, in some cases, since radiation transmitted to the crop can be irregular (at different degree) according to the location within the plot (in our case, IP and UP locations). For example, we can consider that in DAV the daily solar radiation can be representative of the plot, because the cumulative solar radiation evolution is more uniform in space (despite the dynamic intraday patterns), having slight effects on plants located at different points (or rows), while in fixed panels, this condensed value cannot be representative to estimate crop growth in all the plot (with potential differences between plants depending on their position), as shown in Section 3.1.

The inclusion of temporal discretization to improve the simulation of crop development in stressed conditions may be particularly interesting, for example by implementing a mechanistic approach to estimate photosynthesis and respiration processes at a timescale of a few minutes or hours to influence (and improve) prediction at a daily or seasonal scale. This may be useful to (i) optimize water and biomass crop production that can contribute to minimizing crop yield losses related to shading and (ii) to adapt these systems to any water context by controlling both, panels (design or control) and irrigation. Finally, the distinction between diffuse and direct radiation, which was not considered in our experiments, is another perspective to improve photosynthesis modelling.

5. Conclusions and perspectives

In our experimental study, it has been demonstrated that the maize crop growth and production responded to both independent stresses studied here (shade and deficit irrigation) in a combined but not cumulative way, compared to no-stress conditions (full-sun and fully irrigated). In general, a delay of crop development and a significant decrease in leaf area index, total dry matter and grain yield were observed in stressed conditions. Regarding water use in AV systems studied here, we can conclude that shade has an interesting potential to increase irrigation water productivity (in both fully and deficit irrigated conditions) by reducing the water inputs (by up to 19–47% compared to unshaded plots under fully irrigated conditions) and by managing soil moisture (particularly in dynamic DAV systems). Thus, even if AV systems decrease crop yield, these systems have the potential to save water, especially in water-limited systems. An innovative finding in terms of phenology was a strong association of leaf appearance to radiation, showed by an observed increase of phyllochron under shade. Due to the slight impact of panels on air temperature and thermal time, we consider that crop growth and production processes were probably more influenced by shading effects, exposing the relevance of radiative climate in phenology monitoring in AV systems. We then suggested that radiation may be included (in complement to thermal time) in phyllochron estimation in AV systems, particularly in crop modelling studies. Additionally, we did not observe a clear difference in leaf appearance (phyllochron) or leaf canopy area (LAI) between fixed and dynamic AV systems, concluding that the crop phenology and vegetative growth is more affected by the total irradiance received during the daytime that by the intraday dynamics of this radiation.

Another interesting conclusion is that at the leaf level, the responses studied here (stomatal conductance, net assimilation rate of CO2 and leaf temperature) reacted in a well-correlated way to photosynthetically active radiation. This behavior opens new opportunities to optimize water use and shading strategies in further research by using a modelling approach. Crop modelling can be a valuable tool to assess numerous scenarios in silico, crossing the two principal drivers studied here: shading rate and irrigation, and applying these stresses in shade and/or in water-tolerant stages of maize, to find the "good" combination that could tackle the optimization target. However, adaptations of current formalisms may be implemented to consider the specific effects of intermittent shade in the crop processes at plot and leaf scales. Also, specifically in the case of water budget modelling, the most frequently used crop models may be limited regarding their ability to simulate *ETo* as showed by Kimball et al. (2019), constraining the accurate analysis of water fluxes.

Declaration of Competing Interest

The authors declare that they have no known competing financial interests or personal relationships that could have appeared to influence the work reported in this paper.

Data availability

The data that has been used is confidential.

Acknowledgments

This work is part of the R&D project "Sun'Agri 3", supported by the PIA 2 (Programme d'investissement d'avenir) and ANRT (Association nationale de la recherche et de la technologie), under the ADEME (Agence de l'environnement et de la maîtrise de l'énergie) Grant Agreement N°1782C0103. A special thanks to all the technical team of the experimental site of Lavalette (Montpellier) for their invaluable work in all the data acquisition, as well as to the different students involved in the project during their internships.

Appendix A. Supporting information

Supplementary data associated with this article can be found in the online version at doi:10.1016/j.agwat.2023.108187.

References

Abendroth L.J.et al., 2011. Corn growth and development. Iowa State University.
AL-agele, H.A., Proctor, K., Murthy, G., Higgins, C., 2021. A case study of tomato (solanum lycopersicon var. legend) production and water productivity in agrivoltaic systems. Sustainability 13, 2850. https://doi.org/10.3390/su13052850.
Allen, R.G., Pereira, L.S., Raes, D., Smith, M., 1998. FAO Irrigation and drainage, 56. Food and Agriculture Organization of the United Nations, Rome, e156.
Amaducci, S., Yin, X., Colauzzi, M., 2018. Agrivoltaic systems to optimize land use for electric energy production. Appl. Energy 220, 545–561. https://doi.org/10.1016/j.apenergy.2018.03.081.
Andrade, F.H., Ferreiro, M.A., 1996. Reproductive growth of maize, sunflower and soybean at different source levels during grain filling. Field Crops Res. 48, 155–165. https://doi.org/10.1016/S0378-4290(96)01017-9.
Armstrong, A., Ostle, N.J., Whitaker, J., 2016. Solar park microclimate and vegetation management effects on grassland carbon cycling. Environ. Res. Lett. 11, 074016 https://doi.org/10.1088/1748-9326/11/7/074016.
Barron-Gafford, G.A., Pavao-Zuckerman, M.A., Minor, R.L., Sutter, L.F., Barnett-Moreno, I., Blackett, D.T., Thompson, M., Dimond, K., Gerlak, A.K., Nabhan, G.P., Macknick, J.E., 2019. Agrivoltaics provide mutual benefits across the food–energy–water nexus in drylands. Nat. Sustain 2, 848–855. https://doi.org/10.1038/s41893-019-0364-5.
Basso, B., Ritchie, J., 2014. Temperature and drought effects on maize yield. Nat. Clim. Change 4. https://doi.org/10.1038/nclimate2139.
Birch, C.J., Vos, J., Kiniry, J., Bos, H.J., Elings, A., 1998. Phyllochron responds to acclimation to temperature and irradiance in maize. Field Crops Res. 59, 187–200. https://doi.org/10.1016/S0378-4290(98)00120-8.
Blonder, B., Michaletz, S.T., 2018. A model for leaf temperature decoupling from air temperature. Agric. . Meteorol. 262, 354–360. https://doi.org/10.1016/j.agrformet.2018.07.012.
Bonelli, L.E., Monzon, J.P., Cerrudo, A., Rizzalli, R.H., Andrade, F.H., 2016. Maize grain yield components and source-sink relationship as affected by the delay in the sowing date. Field Crops Res 198, 215–225. https://doi.org/10.1016/j.fcr.2016.09.003.
Brisson, N., King, D., Nicoullaud, B., Ruget, F., Ripoche, D., Darthout, R., 1992. A crop model for land suitability evaluation a case study of the maize crop in France. Eur. J. Agron. 1, 163–175. https://doi.org/10.1016/S1161-0301(14)80066-X.
Campos, H., Cooper, M., Habben, J.E., Edmeades, G.O., Schussler, J.R., 2004. Improving drought tolerance in maize: a view from industry. Field Crops Res., Link. Funct. Genom. Physiol. Glob. Change Res. 90, 19–34. https://doi.org/10.1016/j.fcr.2004.07.003.
Chekired, F., Richa, A., Touil, S., Bingwa, B., 2022. Energy yield evaluation of a rainwater harvesting system using a novel agrophotovoltaics design. Desalin. Water Treat. 255, 25–27. https://doi.org/10.5004/dwt.2022.28318.
Chopard, J., 2021. Crop modelling under solar panels: relevance of detailed radiative climate characterization. Itk. Oral. Present.
Earley, E.B., Miller, R.J., Reichert, G.L., Hageman, R.H., Seif, R.D., 1966. Effect of shade on maize production under field conditions1. Crop Sci. 6. https://doi.org/10.2135/cropsci1966.0011183X000600010001x.
Earley, E.B., Mcllrath, W.O., Seif, R.D., Hageman, R.H., 1967. Effects of Shade applied at different stages of plant development on Corn (Zea mays L.) production. Crop Sci. 7. https://doi.org/10.2135/cropsci1967.0011183X000700020018x.
Edmeades, G.O., Bolaños, J., Elings, A., Ribaut, J.-M., Bänziger, M., Westgate, M.E., 2000. The Role and Regulation of the Anthesis-Silking Interval in Maize. Physiology and Modelling Kernel Set in Maize. John Wiley & Sons, Ltd, pp. 43–73. https://doi.org/10.2135/cssaspecpub29.c4.
Elamri, Y., Cheviron, B., Lopez, J.-M., Dejean, C., Belaud, G., 2018. Water budget and crop modelling for agrivoltaic systems: Application to irrigated lettuces. Agric. Water Manag. 208, 440–453. https://doi.org/10.1016/j.agwat.2018.07.001.
Elamri, Y., Cheviron, B., Mange, A., Dejean, C., Liron, F., Belaud, G., 2018b. Rain concentration and sheltering effect of solar panels on cultivated plots. Hydrol. Earth Syst. Sci. 22, 1285–1298. https://doi.org/10.5194/hess-22-1285-2018.
Ephrath, J., Wang, R., Terashima, K., Hesketh, J., Huck, M., Hummel, J., 1993. Shading effects on soybean and corn. Biotronics 22, 15–24.
FAOSTAT, 2022. Statistical Database of the Food and Agriculture Organization of the United Nations. FAO, Rome. ⟨https://www.fao.org/statistics/en/⟩. Accessed 30 June 2022.
Foley, J.A., Ramankutty, N., Brauman, K.A., Cassidy, E.S., Gerber, J.S., Johnston, M., Mueller, N.D., O'Connell, C., Ray, D.K., West, P.C., Balzer, C., Bennett, E.M., Carpenter, S.R., Hill, J., Monfreda, C., Polasky, S., Rockström, J., Sheehan, J., Siebert, S., Tilman, D., Zaks, D.P.M., 2011. Solutions for a cultivated planet. Nature 478, 337–342. https://doi.org/10.1038/nature10452.
Gao, J., Shi, J., Dong, S., Liu, P., Zhao, B., Zhang, J., 2017. Grain yield and root characteristics of summer maize (Zea mays L.) under shade stress conditions. J. Agron. Crop Sci. 203, 562–573. https://doi.org/10.1111/jac.12210.
Givnish, T., 1988. Adaptation to sun and shade: a whole-plant perspective. Funct. Plant Biol. 15, 63–92. https://doi.org/10.1071/PP9880063.
Grillakis, M.G., 2019. Increase in severe and extreme soil moisture droughts in Europe under climate change. Sci. Total Environ. 660, 1245–1255. https://doi.org/10.1016/j.scitotenv.2019.01.001.

Hall, A.J., Lemcoff, J.H., Trapani, N., 1971. Water stress before and during flowering in maize and its effects on yield, its components, and their determinants. Maydica (Italy).

Hirth, M., Dietzel, L., Steiner, S., Ludwig, R., Weidenbach, H., and, J.P., Pfannschmidt, T., 2013. Photosynthetic acclimation responses of maize seedlings grown under artificial laboratory light gradients mimicking natural canopy conditions. Front. Plant Sci. 4, 334. https://doi.org/10.3389/fpls.2013.00334.

Huang, R., Birch, C., George, D., 2011. Water use efficiency in maize production - the challenge and improvement strategies. Proc. 6th Trienn. Conf., Maize Assoc. Aust.

Ion, V., Dicu, G., Dumbravă, M., Temocico, G., Alecu, I.N., Băşa, A.G., State, D., 2015. Harvest index at maize in different growing conditions. Rom. Biotechnol. Lett. 20, 10951.

Jia, S., Li, C., Dong, S., Zhang, J., 2011. Effects of shading at different stages after anthesis on maize grain weight and quality at cytology level. Agric. Sci. China 10, 58–69. https://doi.org/10.1016/S1671-2927(11)60307-6.

Juillion, P., Lopez, G., Fumey, D., Lesniak, V., Génard, M., Vercambre, G., 2022. Shading apple trees with an agrivoltaic system: Impact on water relations, leaf morphophysiological characteristics and yield determinants. Sci. Hortic. 306, 111434 https://doi.org/10.1016/j.scienta.2022.111434.

Kang, S., Shi, W., Zhang, J., 2000. Improved water-use efficiency for maize grown under regulated deficit irrigation. Field Crops Res 67, 207–214. https://doi.org/10.1016/S0378-4290(00)00095-2.

Kawano, K., 1990. Harvest index and evaluation of major food crop cultivars in the tropics. Euphytica 46, 195–202. https://doi.org/10.1007/BF00027218.

Kimball, B.A., Boote, K.J., Hatfield, J.L., Ahuja, L.R., Stockle, C., Archontoulis, S., Baron, C., Basso, B., Bertuzzi, P., Constantin, J., Deryng, D., Dumont, B., Durand, J.-L., Ewert, F., Gaiser, T., Gayler, S., Hoffmann, M.P., Jiang, Q., Kim, S.-H., Lizaso, J., Moulin, S., Nendel, C., Parker, P., Palosuo, T., Priesack, E., Qi, Z., Srivastava, A., Stella, T., Tao, F., Thorp, K.R., Timlin, D., Twine, T.E., Webber, H., Willaume, M., Williams, K., 2019. Simulation of maize evapotranspiration: an inter-comparison among 29 maize models. Agric. . Meteorol. 271, 264–284. https://doi.org/10.1016/j.agrformet.2019.02.037.

Kiniry, J.R., Bonhomme, R., 1991. Predicting maize phenology. Predict. Crop Phenol. 11, 5–131.

Loomis, R.S., Connor, D.J., 1992. Crop Ecology: Productivity and Management in Agricultural Systems, 1st ed. Cambridge University Press. https://doi.org/10.1017/CBO9781139170161.

Mamun, M.A.A., Dargusch, P., Wadley, D., Zulkarnain, N.A., Aziz, A.A., 2022. A review of research on agrivoltaic systems. Renew. Sustain. Energy Rev. 161, 112351 https://doi.org/10.1016/j.rser.2022.112351.

Marrou, H., Guilioni, L., Dufour, L., Dupraz, C., Wery, J., 2013a. Microclimate under agrivoltaic systems: Is crop growth rate affected in the partial shade of solar panels?, 08-15 Agric. . Meteorol. 177, 117–132. https://doi.org/10.1016/j.agrformet.2013.04.012.

Marrou, H., Wery, J., Dufour, L., Dupraz, C., 2013b. Productivity and radiation use efficiency of lettuces grown in the partial shade of photovoltaic panels. Eur. J. Agron. 44, 54–66. https://doi.org/10.1016/j.eja.2012.08.003.

Mbewe, D.M.N., Hunter, R.B., 1986. The effect of shade stress on the performance of corn for silage versus grain. Can. J. Plant Sci. 66, 53–60. https://doi.org/10.4141/cjps86-007.

Meidner, H., Mansfield, T.A., 1965. Stomatal responses to illumination. Biol. Rev. 40, 483–508. https://doi.org/10.1111/j.1469-185X.1965.tb00813.x.

Nesmith, D.S., Ritchie, J.T., 1992. Effects of soil water-deficits during tassel emergence on development and yield component of maize (Zea mays). Field Crops Res. 28, 251–256. https://doi.org/10.1016/0378-4290(92)90044-A.

Otegui, Bonhomme, 1998. Grain yield components in maize. I. Ear growth and kernel set. Field Crop Res. 56, 247–256.

Oumarou Abdoulaye, A., Lu, H., Zhu, Y., Alhaj Hamoud, Y., Sheteiwy, M., 2019. The global trend of the net irrigation water requirement of maize from 1960 to 2050. Climate 7, 124. https://doi.org/10.3390/cli7100124.

Padilla, J.M., Otegui, M.E., 2005. Co-ordination between leaf initiation and leaf appearance in field-grown maize (zea mays): genotypic differences in response of rates to temperature. Ann. Bot. 96, 997–1007. https://doi.org/10.1093/aob/mci251.

Pantin, F., Simonneau, T., Rolland, G., Dauzat, M., Muller, B., 2011. Control of leaf expansion: a developmental switch from metabolics to hydraulics. Plant. Physiol. 156, 803–815. https://doi.org/10.1104/pp.111.176289.

Pearcy, R.W., Gross, L.J., He, D., 1997. An improved dynamic model of photosynthesis for estimation of carbon gain in sunfleck light regimes. Plant, Cell Environ. 20, 411–424. https://doi.org/10.1046/j.1365-3040.1997.d01-88.x.

Poehlman, J.M., 2013. Breeding Field Crops. & Business Media. Springer Science.

Reed, A.J., Singletary, G.W., Schussler, J.R., Williamson, D.R., Christy, A.L., 1988. Shading effects on dry matter and nitrogen partitioning, kernel number, and yield of maize. Crop Sci. 28. https://doi.org/10.2135/cropsci1988.0011183X002800050020x.

Reilly, J.M., 2002. Agriculture: The Potential Consequences Of Climate Variability And Change For The United States, 1. Published. Cambridge University Press, Cambridge.

Ren, B., Cui, H., Camberato, J.J., Dong, S., Liu, P., Zhao, B., Zhang, J., 2016. Effects of shading on the photosynthetic characteristics and mesophyll cell ultrastructure of summer maize. Sci. Nat. 103, 67. https://doi.org/10.1007/s00114-016-1392-x.

Retkute, R., Smith-Unna, S.E., Smith, R.W., Burgess, A.J., Jensen, O.E., Johnson, G.N., Preston, S.P., Murchie, E.H., 2015. Exploiting heterogeneous environments: does photosynthetic acclimation optimize carbon gain in fluctuating light? J. Exp. Bot. 66, 2437–2447. https://doi.org/10.1093/jxb/erv055.

Sage, R.F., McKown, A.D., 2006. Is C4 photosynthesis less phenotypically plastic than C3 photosynthesis? J. Exp. Bot. 57, 303–317. https://doi.org/10.1093/jxb/erj040.

dos Santos, C.L., Abendroth, L.J., Coulter, J.A., Nafziger, E.D., Suyker, A., Yu, J., Schnable, P.S., Archontoulis, S.V., 2022a. Maize Leaf Appearance Rates: A Synthesis From the United States Corn Belt. Front. Plant. Sci. 13. https://doi.org/10.3389/fpls.2022.872738.

Shen, Y., Oki, T., Utsumi, N., Kanae, S., Hanasaki, N., 2008. Projection of future world water resources under SRES scenarios: water withdrawal / Projection des ressources en eau mondiales futures selon les scénarios du RSSE: prélèvement d'eau. Hydrol. Sci. J. 53, 11–33. https://doi.org/10.1623/hysj.53.1.11.

Siebert, S., Döll, P., 2010. Quantifying blue and green virtual water contents in global crop production as well as potential production losses without irrigation. J. Hydrol. Green. -Blue Water Initiat. (GBI) 384, 198–217. https://doi.org/10.1016/j.jhydrol.2009.07.031.

Tahir, Z., Butt, N.Z., 2022. Implications of spatial-temporal shading in agrivoltaics under fixed tilt & tracking bifacial photovoltaic panels. Renew. Energy 190, 167–176. https://doi.org/10.1016/j.renene.2022.03.078.

Tilman, D., Cassman, K.G., Matson, P.A., Naylor, R., Polasky, S., 2002. Agricultural sustainability and intensive production practices. Nature 418, 671–677. https://doi.org/10.1038/nature01014.

Tollenaar, M., 1977. Sink-source relationships during reproductive development in maize. A review. Maydica 22, 49–75.

Valle, B., 2017. Modélisation et optimisation de la croissance de la laitue dans un système agrivoltaïque dynamique. Ph. D. thesis, Montpellier SupAgro. ⟨https://www.theses.fr/2017NSAM0017⟩.

Verheul, M.J., Picatto, C., Stamp, P., 1996. Growth and development of maize (Zea mays L.) seedlings under chilling conditions in the field. Eur. J. Agron. 5, 31–43. https://doi.org/10.1016/S1161-0301(96)02007-2.

Wang, D., Sun, Y., 2018. Optimizing light environment of the oblique single-axis tracking agrivoltaic system. IOP Conf. Ser.: Earth Environ. Sci. 170, 042069 https://doi.org/10.1088/1755-1315/170/4/042069.

Weselek, A., Ehmann, A., Zikeli, S., Lewandowski, I., Schindele, S., Högy, P., 2019. Agrophotovoltaic systems: applications, challenges, and opportunities. A review. Agron. Sustain. Dev. 39, 35. https://doi.org/10.1007/s13593-019-0581-3.

Yuan, L., Liu, J., Cai, Z., Wang, H., Fu, J., Zhang, Hongtao, Zhang, Y., Zhu, S., Wu, W., Yan, H., Zhang, Hui, Li, T., Zhang, L., Yuan, M., 2021. Shade stress on maize seedlings biomass production and photosynthetic traits. Cienc. Rural 52. https://doi.org/10.1590/0103-8478cr20201022.

Zhang, G.-P., Marasini, M., Li, W.-W., Zhang, F.-L., 2022. Grain filling leads to backflow of surplus water in maize grain via the xylem to the cob and plant. BioRxiv. https://doi.org/10.1101/2022.07.22.501090.

Zhang, J., Dong, S., Wang, K., Hu, C., Liu, P., 2006. Effects of shading on the growth, development and grain yield of summer maize. Ying yong sheng tai xue bao = J. Appl. Ecol. 17 (4), 657–662.

Zou, Y., Saddique, Q., Ali, A., Xu, J., Khan, M.I., Qing, M., Azmat, M., Cai, H., Siddique, K.H.M., 2021. Deficit irrigation improves maize yield and water use efficiency in a semi-arid environment. Agric. Water Manag. 243, 106483 https://doi.org/10.1016/j.agwat.2020.106483.